Journal of Membrane Science 486 (2015) 71–88

Contents lists available at ScienceDirect

Journal of Membrane Science

journal homepage: www.elsevier.com/locate/memsci

Review

Potential ion exchange membranes and system performance in reverse electrodialysis for power generation: A review

Jin Gi Hong [a,1], Bopeng Zhang [a,1], Shira Glabman [a], Nigmet Uzal [a,b], Xiaomin Dou [a,c], Hongguo Zhang [a], Xiuzhen Wei [a], Yongsheng Chen [a,*]

[a] School of Civil and Environmental Engineering, Georgia Institute of Technology, Atlanta, GA 30332, United States
[b] Faculty of Engineering and Natural Sciences, Department of Environmental Engineering, Abdullah Gul University, Kayseri 38039, Turkey
[c] School of Environmental Science and Engineering, Beijing Forestry University, Beijing 100083, PR China

ARTICLE INFO

Article history:
Received 23 September 2014
Received in revised form
17 February 2015
Accepted 24 February 2015
Available online 12 March 2015

Keywords:
Renewable energy
Ion exchange membranes
Reverse electrodialysis
Salinity gradient power
Electrochemical properties

ABSTRACT

Reverse electrodialysis (RED) is an emerging membrane-based energy conversion process used to extract electricity by mixing two water streams of different salinities. This technique utilizes transport of cations and anions during controlled mixing of saltwater and freshwater through selective ion exchange membranes. The development of ion exchange membranes and optimization of system performance are crucial for sustainable energy capture from salinity gradients using RED. Recently, increased attention has been given to the preparation of ion exchange membranes and to understanding the factors that determine the RED power performance. This review evaluates potential ion exchange membrane materials, currently available state-of-the-art RED membranes, and their key properties. Discussion will focus on the electrochemical and physical properties of these membranes (e.g., resistance, permselectivity, and swelling) because of their significant role in RED performance throughout the system. Although an interconnected relationship exists between membrane properties, RED requires high quality membranes that are uniquely tailored to have a low resistance and high permselectivity. Moreover, harnessing this potential technology demands not only carefully optimized components but also a novel RED stack design and system optimization. The key findings and advancements needed to assure proper stack design and optimization are also described. This review paper's goal is to elucidate effective energy conversion from salinity gradients and expedite implementation of RED as the next promising renewable source of power for large-scale energy generation.

Contents

* Corresponding author. Tel.: +1 404 894 3089.
E-mail address: yongsheng.chen@ce.gatech.edu (Y. Chen).
[1] The first and second authors contributed equally to this work.

http://dx.doi.org/10.1016/j.memsci.2015.02.039
0376-7388/

1. Introduction

The development of renewable and sustainable energy conversion technology is widely recognized as an important strategy for global energy security and is becoming extremely important due to growing environmental concerns, such as pollution and global warming. The ocean is a largely untapped renewable and clean energy resource. Mixing ocean water with freshwater creates free energy. More specifically, the chemical potential of sea and river water can be converted into electrical energy. The amount of available energy due to the salinity gradient of seawater mixed with river water is equivalent to the energy obtained from a waterfall that is ~270 m high [1–3]. Salinity gradient energy has become recognized as a nonpolluting and sustainable energy source, and its viability is further assured by the abundance of river and seawater. The two most promising approaches in capturing salinity gradient energy are (1) pressured-retarded osmosis (PRO), a membrane technology using semi-permeable membranes and (2) reverse electrodialysis (RED), which uses ion exchange membranes (IEMs). Each of these technologies is used in different salinity conditions. For example, mixing concentrated brines is suitable for PRO, and mixing sea and river water is favorable for RED [4]. Another possible salinity gradient energy source is obtainable by incorporating wastewater effluent with brines discharged from desalination plants; however, this technology needs more membrane and system optimization. The successful application of PRO and RED are often limited by the cost of membranes. Also, the performance deterioration of membranes is an obstacle for commercialization. The membranes used in PRO and RED are in various stages of development. Compared to the availability of semi-permeable membranes used in PRO, the access to RED ion exchange membranes is relatively low. In addition, commercially developed and optimized membranes for RED application are rare primarily because the currently available IEMs were developed specifically for electrodialysis (ED). Fig. 1 shows how ED converts salt water to fresh water whereas RED uses both salt water and fresh water to create energy or voltage. Hence, RED is the inverse process of ED.

Both ED and RED use the ion exchange process to achieve their goals, and they both consist of an alternating series of anion exchange membranes (AEMs) and cation exchange membranes (CEMs) as shown in Fig. 2.

The principle of ED was first demonstrated in 1890 by Maigrot and Sabates with the initial aim of demineralizing sugar syrup [5]. The principle of RED was first developed in 1954 by Pattle [2], who proved that mixing river water with seawater can be used as a power source. Weinstein et al. [6] proved RED power generation feasible by using a simple mathematical model that emphasized the importance of manufacturing RED IEMs and optimizing their operating conditions to advance RED technology for large-scale energy conversion. In 1980, Lacey [7] concluded that membranes with low electrical resistance and high selectivity are necessary to maximize the net output voltage from RED cells. Lacey also stated that RED membranes should be durable, physically strong, and dimensionally stable for the lowest possible cost. Jagur-Grodzinski et al. [8] investigated the role of flow control using spacer patterns to generate higher power. In 2007, Turek and Bandura [9] noted that the membrane size with shorter length, but wider width (i.e., shorter ionic flow path) results in more effective energy production in the industrial unit.

Daniilidis et al. [10] also emphasized that affordable membrane cost in combination with power performance is the key to successful RED commercialization. The current cost of IEMs is 2–3 times higher than that of reverse osmosis (RO) membranes used in desalination processes [1,11]; however, cost reduction is possible as global demand increases. In the last decade, RO membranes have had a notable cost reduction owing to significant development in membrane materials and fabrication methods, resulting in an increased use of RO for water desalination application. Likewise, proper IEM development for RED is necessary to promote stable power generation in an RED cell.

Recently, some efforts have been reported on designing RED IEMs that show the potential of IEM development for viable energy production [12–15]. These studies focus on investigating the core electrochemical and physical properties of IEMs that directly influence RED performance. Even though this research has provided key performance-determining membrane properties in an RED stack, further physico- and electrochemical property analyses are needed. Research on exchange capacity, permselectivity, and resistance is needed to provide a greater variety of membranes prepared with different methods and materials to improve real power density generation.

Since RED membrane development and optimization are rapidly transitioning and becoming more common for practical application, it is worthwhile to present an overview of IEMs for RED. This includes a review of emerging membrane materials, preparation methods, properties, and other relevant components of an RED stack. Other topics include potential RED IEM materials and current state-of-the-art membranes for RED application. The final focus will be on the authors' investigation of key physical and electrochemical properties of ideal RED membranes essential to system performance based on experimentally determined results and theoretical modeling approaches.

2. Key membrane properties and performance in RED

The study of IEM properties examines how they affect IEM performance under different circumstances [16,17]. The durability of membrane material and fine physicochemical characteristics are of great importance in many applications. Thermal and chemical stabilities are good indicators of the durability of membranes. Transport-related properties, such as swelling degree, permselectivity, ion exchange capacity (IEC), and ionic conductivity influence the electrochemical characteristics. Most of these properties can

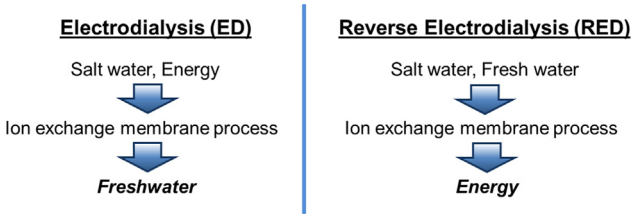

Fig. 1. Simplified scheme flow for ED and RED processes.

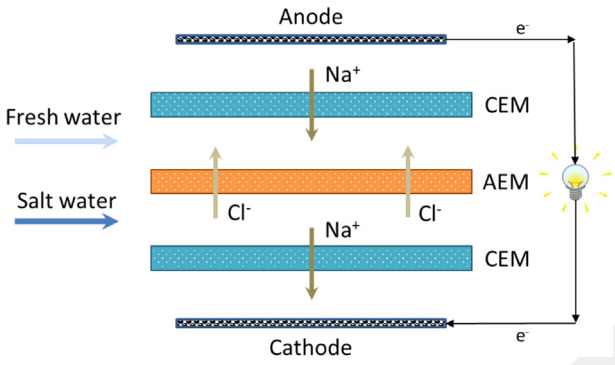

Fig. 2. Simplified schematic representation of an RED cell.

be determined experimentally. The rest of them can be calculated based on their relationship with other available parameters. It should be noted that the requirement for IEMs in RED applications is different from the requirement for other applications, especially ED applications, because the aim of RED is to generate electrical energy instead of separating substances as in ED [18]. Thus, ionic resistance and permselectivity are the most crucial properties while others that are not related to these two properties weigh less in RED power generation.

2.1. Thermal stability, chemical stability, and mechanical strength

The thermal stability of IEM depends on the crosslinking degree, thermal stability of inert polymers, and reinforcing fabric (e.g., poly(vinyl) chloride and polyethylene). The size of the counter-ion also affects the thermal stability of the membrane [19]. In general, the requirements ensuring thermal stability of IEMs used in RED are not high when compared to thermal stability requirements for more common devices such as fuel cells [20]. The common temperature used for RED systems is generally around room temperature with a possible seasonal variation within 30 K.

Chemical stability depends on the durability of the membrane in various acidic or alkaline solutions. In general, cation exchange members (CEMs) are more durable than anion exchange members (AEMs) in terms of both thermal stability and chemical stability in strongly acidic and strongly alkaline solutions because the quaternary ammonium groups in AEMs tend to decompose at elevated temperatures and in concentrated alkali solutions [17,21].

Chemical stability is important for ED processes because the electricity applied to the system would inevitably dissociate water molecules and generate proton and hydroxyl ions [22]. In specific ED applications, such as acid and base manufacturing, pH change in a solution flow due to IEMs is significant. The chemical stability of IEMs to withstand harsh pH environments is important. In addition, the current density applied in most ED processes will often approach the limiting current density or even reach the over-limit current density range in order to achieve the highest possible reaction rate. The high electrical field in the membrane bulk exerts a relatively strong force onto fixed charges. It is thus crucial to have a high stability of fixed charge groups in the membrane bulk [23]. In the case of RED application, the dissociation of water is limited to a negligible extent on the electrodes, so that pH of the rinse solution is expected to be stable. Feeding solutions (river and salt water) are close to neutral, and no significant process would alter or interfere with the pH throughout the residence time of the solution in each compartment. Consequently, the chemical stability of IEMs is not crucial in RED application [13,16].

Membrane mechanical strength is necessary to maintain good durability under the flow of feed solutions creating hydraulic pressure over the membrane in addition to the osmotic pressure caused by concentration gradient. However, in typical seawater/river water cases, the concentration difference is in the range of 0.01–0.5 M (a bit over an order range). Some ED processing may encounter a gradient of several orders (e.g., deionization). The osmotic pressure exerted onto the membrane is quite different. On the other hand, the mechanical strength of the membrane is not as crucial in the RED system when compared with the PRO technique. In the latter case, membranes have to withstand tremendous hydraulic pressure given a water flux of 20–50 L m^{-2} h^{-1} [24].

The common practice of crosslinking membrane material is very helpful in strengthening it, but crosslinking also tends to increase membrane resistance [17,23]. As will be discussed later, the resistance of the membrane is more important, and it is unproductive to sacrifice resistance in order to improve mechanical strength through cross linking.

2.2. Swelling degree, ion exchange capacity, and fixed charge concentration

The swelling degree of the membrane is usually expressed as water content or water uptake of the membrane under a given condition. The swelling degree is dependent on the nature of the membrane structure and material as well as the outer solution condition [16,25]. IEC represents the number of fixed charges on the membrane in a unit of membrane dry weight. Most CEMs incorporate sulfonic acid ($-SO_3^{2-}$) or carboxylic acid groups ($-COO^-$) in the membrane structure, while ammonium groups ($-NR_3^+$, $-NH_4^+$, $-NH_2$, $=NH$, $\equiv N$) are common in AEMs. The type and distribution of these ion exchange groups classify different membranes. The ion exchange capacity (IEC) of ion exchanges membranes (IEMs) are usually determined experimentally according to the titration method using a strong acid or base of HCl for CEMs and NaOH for AEMs, respectively.

Swelling is usually considered to be an adverse effect because it tends to decrease the permselectivity of ion exchange membranes, but it also decreases the membrane resistance in certain cases, especially for anion exchange membranes [26–28]. For applications such as RED, the loss of permselectivity may not be an adverse effect if a much lower resistance is achieved. For example, Geise et al. [27] made AEMs based on poly(phenylene oxide) and poly(sulfone) polymers. High swelling degrees led to increases in resistance of more than three orders of magnitude, while the permselectivity decreased by only 6%. As will be discussed in the following section, the effect of the decrease of permselectivity on power output would be negligible because power density will increase significantly with a significantly lowered resistance.

A high IEC indicates more ion exchange groups in the membrane bulk, but swelling tends to dilute the concentration of these groups as distance between these ion exchange groups increase when the membrane is immersed in a solution. Therefore, the ratio of IEC and swelling degree, termed as the fixed charge density (or fixed ion concentration), depicts the overall effect of the swelling degree on IEC and provides a direct relationship

between the two electrochemical properties of an IEM [26,29]. The fixed charge density (meq g H_2O^{-1}) is defined in Eq. (1) if the IEC and water uptake of a membrane are known [17,26,30]:

$$\mathrm{FCD} = \frac{\mathrm{IEC}}{w_u} \tag{1}$$

where FCD is the fixed charge density and w_u is the water uptake.

The advantage of using fixed charge density is easily seen when IEC and water content do not change simultaneously. For example, increased IEC is reported to result in higher permselectivity of IEMs [31]; however, the water content in the membrane phase may vary under different solution concentrations due to osmosis deswelling and the decrease of free volume in the membrane phase [32]. As a result, the final membrane may exhibit lower permselectivity with the same IEC because its final fixed charge density is lower. This deswelling effect on the membrane is more pronounced in AEMs than in CEMs [26,27,32,33].

2.3. Ionic resistance and permselectivity

Because the RED system is essentially a dialytic battery, the ionic resistance (or ionic conductivity since ions are actually conducting electricity) of an RED system is analogous to the internal resistance of a battery. As a major part of this internal resistance, the ionic resistance of IEM in the RED system is usually measured experimentally. Similar to the internal resistance of a battery, the ionic resistance determines the energy loss in an operating stack, which affects the power output of the system [26,34].

The determination of membrane resistance is not straightforward because the measurement is usually taken while the membrane is in a solution as encountered in power generation applications; however, conditions such as solution concentration, temperature, concentration gradient across the membrane, and experimental methods, all affect the measurement and its result. This cause and effect relationship necessitates a discussion in detail.

The ionic resistance of membranes is commonly measured using indirect methods (no direct contact of the electrodes and the membrane) in RED research [26,34–37]. The alternative current (AC) is preferable because it avoids electrochemical reactions that may occur during measurement and is more accurate in differentiating the pure membrane resistance from common resistance, including the diffusion boundary layer (DBL) and double-layer effects. Direct current (DC) is also reported to be useful in the resistance measurement [34,36,38]. The membranes to be measured are immersed in sodium chloride or potassium chloride solutions of concentrations of 0.5 M or 1.0 M; however, the resistance may change with different external solutions and under different temperatures [17,35].

In RED application, IEMs divide salt solutions of different concentrations. As a result, the apparent membrane resistance is significantly different from the measured value in a 0.5 M NaCl solution [35,39]. Therefore, a more comprehensive measurement of membrane resistance considering the effect of the external solution concentration is critical in modeling the RED system. Two techniques, namely chronopotentiometry and electrochemical impedance spectroscopy (EIS), have been used to solve the aforementioned difficulties during the membrane resistance measurement.

Chronopotentiometry is widely used to investigate kinetic effects and adsorption during the transport process in IEMs [40,41]. Through chronopotentiometry studies, the time dependence of the concentration gradients and the thickness of DBL under different current density can be determined. Also, the validity of the Nernst–Planck equation and the Donnan theory are also confirmed under transient conditions [40,42]; however, for measuring the double layer and quantifying its electrochemical effect on the membrane, chronopotentiometry is not sufficient.

EIS is a technique used for studying and characterizing the electrical properties of porous materials and can be used to characterize IEMs. EIS provides another perspective in the study of the IEM system by equating the system to an electrical circuit with capacitors and resistors [43,44]. The existence of three sublayers of the IEM system, including the membrane, the electrical double layers, and the DBLs, has been studied using the EIS technique, and the quantitative circuit model has been established [43]. By changing the frequency of the applied AC potential, the resistance of the solution and the electrical double layer can be differentiated [16,36]. For example, when the applied AC frequency is low or when DC is applied to the membrane system, the resulting electrical equivalent circuit indicates the effect of the diffusion layer and the electrical double layers as well as their contribution to the total electrical resistance of the system. Finally, an analysis under a high frequency AC reveals the resistance attributed to the membrane polymer itself [45].

Permselectivity describes the ability of a membrane to prevent co-ions from passing through the membrane. It is measured by transport number and related to the fixed charge concentration of the membrane and the external solution concentration. Theoretically, a perfect IEM would have a permselectivity of one when the complete exclusion of the co-ions from the membrane is achieved; however, according to Donnan's theory, a certain amount of co-ions could contribute to the transport current [33,46]. Thus, the permselectivity would decrease below the ideal value of 1 as the solution concentration increases [17].

In practice, the apparent permselectivity is of more concern in RED because it determines the membrane potential (E_m) achievable under the given circumstances according to the following equation [47]:

$$E_m = \alpha_m \frac{RT}{F} \ln\left(\frac{a_c}{a_d}\right) \tag{2}$$

where α_m is the apparent membrane permselectivity, R is the gas constant (J mol^{-1} K^{-1}), T is the absolute temperature (K), F is the Faraday constant (C mol^{-1}), α_c is the activity (mol L^{-1}) of the concentrated salt solution, and α_d is the activity (mol L^{-1}) of the diluted salt solution.

The relationship between the permselectivity and the ionic resistance of the membrane is complicated because of the interactive effects from fixed charged groups and membrane swelling, as discussed in the previous section. Some researchers have concluded that it is not necessary to achieve both high permselectivity and low ionic resistance because an RED system can tolerate moderate permselectivity. After all, the main goal is to produce electricity and not to separate solutions [26]. The requirement of membrane resistance is stricter for an RED application than an ED application because the improvement of membrane conductivity is a step in the process of optimization; however, efficiency is the major hurdle that a successful RED application must overcome. Thus, membrane resistance is central to this hurdle because it is the key parameter that determines system efficiency. On the other hand, the permselectivity is more important in the ED process, especially for continuous deionization in which the purity of the products is of greater concern [48,49]. This allows the resistance to be sacrificed to some extent. In summary, the development and synthesis of IEMs with well-balanced permselectivity and low resistance is desirable to optimize the RED salinity gradient power generation process [27].

2.4. RED performance

In order to effectively capture the salinity gradient power, an RED stack with 20–50 cells may be necessary [50]. In this type of setup, not only is the performance of the membrane influential,

but other components, including feed solution compartments, electrodes, and spacers have a significant effect. They all cause ionic resistance but to different degrees. As soon as the transport of ions through membranes begins, concentration polarization occurs and affects the overall resistance. The estimation and measurement of power output depends largely on the understanding of these processes and their effects. Furthermore, the successful development of this technology should not only include enhancement of the electrochemical properties of the stack but also optimize other factors including the spacer design, electrode requirements, pumping energy consumption, and pretreatment of the water, to reduce membrane fouling.

2.4.1. Internal resistance of the system

The resistance of an RED stack is the summation of resistances of all components in a series, including electrodes, electrolytes, diffusion boundary layers at the membrane surface, and membranes. Simplified models neglect the resistance of diffusion boundary layers or combine its contribution with membrane resistance and express the overall resistance (Ω) as follows [6,7]:

$$R_{stack} = \frac{N}{A}\left(R_a + R_c + \frac{d_c}{k_c} + \frac{d_d}{k_d}\right) + R_{el} \tag{3}$$

where A is the effective membrane area (cm^2), R_a is the resistance ($\Omega\ cm^2$) of anion exchange membrane, R_c is the resistance ($\Omega\ cm^2$) of cation exchange membrane, R_{el} is the resistance (Ω) of electrodes, d_c is the thickness (cm) of the concentrated solution, d_d is the thickness of diluted solution, κ_c is the specific conductivity ($mS\ cm^{-1}$) of the concentrated solution, and κ_d is the specific conductivity ($mS\ cm^{-1}$) of the diluted solution. The presence of spacers will significantly lower the power output due to the loss of the membrane area from non-conductive spacer blockage [26]. If the spacer shadow effect is considered as the portion of the membrane area masked by the spacer denoted as β, the resistance of the stack can be written as [26,51]

$$R_{stack} = \frac{N}{A}\left(\frac{R_a}{1-\beta} + \frac{R_c}{1-\beta} + \frac{d_c}{k_c} + \frac{d_d}{k_d}\right) + R_{el} \tag{4}$$

However, there is no consensus on the qualification of shadow effect β. An apparent shadow effect can be measured as ratio of experimental power achieved using AC as W_{AC} (W) and the theoretical power achievable W_{theo} (W) in the following equation [30,37]:

$$\beta = \left(1 - \frac{W_{AC}}{W_{theo}}\right) \times 100\% \tag{5}$$

W_{theo} is estimated based on the Nernst equation (Eq. (1)) under the assumption of 100% permselectivity at a given salinity condition. The ratio of a theoretically calculated membrane area to an actual membrane area used in practice is also suggested [22,51]. Then, the resistance of all of the different parts of a cell are multipliable with the exception of the electrodes [50]. The electrode resistance may be considered negligible if the stack is scaled with a large number of cells (e.g., larger than 20 cells) but with only two electrodes [1,52].

A more comprehensive consideration of the stack resistance also includes the diffusion boundary layer and the salinity gradient resistance [53]. Considering all of these effects, the resistance of a RED stack (Ω) of N cells is expressed as

$$R_{stack} = N(R_{ohmic} + R_{\Delta C} + R_{BL}) \tag{6}$$

where R_{ohmic} is the membrane resistance attributed to the ionic transport through the membranes, which is equal to the one cell resistance discussed above. $R_{\Delta C}$ is the resistance attributed to the reduced electromotive forces as a consequence of the change in the concentration of the bulk solution, and R_{BL} is the boundary layer resistance due to concentration polarization.

The $R_{\Delta C}$ considers the change of the solution concentration from the inlet to the outlet of the solution compartment. The result of this concentration gradient is the spatial difference of membrane potential. The resistance due to the concentration change in the bulk solution is expressed as

$$R_{\Delta C} = \frac{V_{stack} - V_{average}}{JA} = \frac{\alpha RT}{FJA} \ln\left(\frac{1 + \frac{JL}{Fq_d c_d}}{1 - \frac{JL}{Fq_c c_c}}\right) \tag{7}$$

where J is the current density ($A\ m^{-2}$), α is the average apparent permselectivity of the membrane (%), c_c is the concentration ($mol\ L^{-1}$) of the concentrated salt solution, and c_d is the concentration ($mol\ L^{-1}$) of the diluted salt solution, q_c and q_d are the flow rate ($m^3\ s^{-1}$) of the concentrated and diluted solutions, respectively, and L is the cell length (m). Thus, the stack resistance is connected with the electricity current and the hydrodynamic environment in the system.

The summation of resistance from all components is an effective representation of the entire RED stack resistance; however, in a real RED application, possible errors of resistance estimation, specifically in IEMs and solution compartments, may occur when the feed solution concentration is different from the concentration when the resistance measurement was taken, as discussed in Section 2.3. For example, the apparent resistance of IEMs in a stack is significantly higher than the value from the standard measurement (with 0.5 M NaCl solution) [35,36,39]. Thus, the effect of changing resistance needs to be clarified and modeled for an improved representation of the RED stack.

One proposed explanation compares the membrane resistance with the resistance due to concentration polarization, which adequately accounts for its concentration dependency [26,35]. This will be discussed in more detail in the next section. A decrease in resistance is reported when the solution flow rate increases. This supports the theory because the resistance due to concentration polarization can be largely avoided or eliminated altogether when the proper agitation of electrolytes is maintained by providing a sufficient flow [26,35,40,42].

Several models have been proposed based on experimental data. For example, Veerman [50] fitted experimental data to an exponential function in the form of

$$R_m = A + B \cdot e^{-rC} \tag{8}$$

where A, B, and r are all fitting parameters, and C is the solution concentration.

Later, Kim et al. [54] pointed out that membrane resistance is a linear function of the reciprocal of a solution concentration:

$$R_m \propto \frac{1}{C} \tag{9}$$

The most recent development on this topic proposed the modified relationship as [39]

$$R_m = A + \frac{r}{C} \tag{10}$$

where A and r are constants to be fitted from experimental data. The last model fits well and partly explains the phenomenon found by Guler et al. [30] that when the membrane thickness becomes smaller and smaller, the membrane resistance does not extrapolate to zero. More efforts are needed to further explore the physical meanings behind these empirical models.

Finally, the resistance of feed solutions, particularly from the diluted solution, decreases as the compartment thickness decreases. The resistance of the fresh water compartment has significant weight [35,50]. One obvious approach to decrease stack resistance would be to decrease the compartment thickness. If both compartments are decreased, the resistance can be

significantly lowered, but the pumping energy is further increased at the same time [18]. Several designs of RED stacks using different thicknesses of spacers in concentrated and diluted compartments have been reported in literature as well [7,55]. If the diluted compartment uses thinner spacers (i.e., shorter intermembrane distance) than concentrated compartments, the system resistance could effectively be reduced as well as require less pumping energy for the entire system [6,55]; however, a stack with different compartment thicknesses may suffer bulging caused by the pressure difference [9]. Another approach to decrease the resistance from the diluted compartment is based on the fact that the conductivity of a solution increases with an increasing concentration. If the concentration within the diluted compartment is increased, the resistance will be lowered. This is exactly the approach taken to utilize brine water as a high concentration feed and brackish or seawater as a low concentration feed [56,57]. In this case, the water resource is not as widely available as it is when using seawater and river water. In summary, research efforts should be focused on novel approaches to decrease the resistance of solution compartments while requiring moderate pumping energy consumption in order to optimize system efficiency.

2.4.2. Concentration polarization

Concentration polarization arises essentially because of the different transport number of ions in the bulk solution and in the membrane phase. The transport number in the membrane phase for counter-ions is higher than in the solution phase. Consequently, the depletion of counter-ions at the membrane–solution interface surpasses the feed speed from the solution bulk. A concentration gradient gradually forms as the transport of ions (i.e., the passage of ionic current) continues as it also does in an ED stack [33,58,59].

The widely used DC method in the measurement of membrane resistance may include the contribution DBL resistance due to concentration polarization because the method essentially determines the sum of the membrane resistances and the DBL resistance. Therefore, in a RED system, the stack resistance acquired experimentally under the standard condition (i.e., 0.5 M NaCl solution) often fails to predict the accurate power output when there is a current flowing between electrodes, as discussed in the previous section. This deviation is more pronounced in the fresh water compartment [29,43].

One approach in quantifying the concentration polarization follows the original study conducted in the ED field by Barragan et al. [60]. The change in the resistance is usually considered as ohmic and non-ohmic parts, which are due to solution conductivity change and membrane potential change, respectively [60]. Brauns [56] assumed a linear concentration gradient from the bulk solution to the membrane–solution interface at a steady state [56]. Then, the ohmic resistance that resulted from the change of solution concentration can be calculated using the average concentration at the DBL layer:

$$R_{ohmic} = \frac{\delta}{\left(\frac{c_b + c_i}{2}\right) \cdot \Lambda_b} \tag{11}$$

where c_b and c_i are the concentrations (mol L^{-1}) of the bulk solution and the solution at the interface, respectively, Λ_b is the molar conductivity (S m^{-1} mol^{-1}) of the bulk solution, and δ is the thickness (m) of the boundary layer [56]. A more precise way to estimate the same resistance is by integrating along the DBL thickness [60]:

$$R_{ohmic} = \frac{1}{\Lambda_b} \int_0^{\delta} \left(\frac{1}{c(x)} - \frac{1}{c_b} \right) dx \tag{12}$$

where $c(x)$ is the concentration of solution at a certain point within the boundary layer. The concentration at the membrane–solution interface c_i is estimated with respect to the limiting current density i_l (A m^{-2}) [40] expressed as

$$c_i = c_b \cdot \left(1 - \frac{i}{i_l}\right) \tag{13}$$

where i is the current density (A m^{-2}) in the system. It is important to note that even though the operating condition of RED has a current density far below the limiting current, the concept of the limiting current is still important for the estimation of DBL thickness and DBL resistance. The key parameters, such as the limiting current density and the thickness of DBL, can be determined using techniques such as chronopotentiometry and EIS, as discussed in Section 2.3. For the non-ohmic resistance due to membrane potential change, the same techniques are also applicable, and are widely used in the study of non-ohmic resistance due to concentration polarization [18,38,39,61].

The situation becomes more complicated when the flow of water in the cell compartments affects the hydrodynamic environment of the DBL, which also affects the thickness and concentration at the solution-membrane interface. For example, Vermaas et al. [62] developed a model assuming that the boundary layer resistance is proportional to the velocity shear at the membrane–solution interface [62]. The R_{DBL} is

$$R_{DBL} \propto \frac{h}{v_{average}} = t_{res}\frac{h}{L} \tag{14}$$

where $v_{average}$ is the average velocity (m s^{-1}), t_{res} is the residence time (s), L is the cell length (m), and h is the cell thickness (m). When the flow distribution within the solution compartment is considered, Eq. (13) can only estimate the DBL on an average basis [63]. Furthermore, the slight dependence of DBL resistance on current density is not considered in this hydraulic relationship; however, in the classical ED theory, the effect of current density on resistance is well-quantified, as seen in Eq. (13) [60]. Recently, researchers have taken these processes into account and provided more accurate simulations on system resistance and power generation [64,65].

2.4.3. Power output

The theoretical salinity gradient power generation in an RED system with many cells has long been reported based on Kirchhoff's law and based on the fact that the potential generated from different cells is additive [6]. The stack of N membrane pairs generates an open-circuit potential of V_{stack} (V), which can be calculated as

$$V_{stack} = 2N\frac{\alpha RT}{F}\ln\left(\frac{a_c}{a_d}\right) \tag{15}$$

where N is the number of stacks, R is the gas constant (J mol^{-1} K^{-1}), T is the absolute temperature (K), F is the Faraday constant (C mol^{-1}), α is the average apparent permselectivity of the membranes (%) in the stack, a_c is the activity (mol L^{-1}) of the concentrated salt solution, and a_d is the activity (mol L^{-1}) of the diluted salt solution.

According to Kirchhoff's law, the power output (W) of the RED stacks is calculated as

$$W = I^2 R_L = \frac{V_{stack}^2 R_L}{(R_{stack} + R_L)^2} \tag{16}$$

The power output is a function of overall stack resistance R_{stack} (Ω) and external load resistance R_L (Ω), so the output power, W (W), is maximized when R_{stack} and R_L are equal [6,7], written as

$$W_{max} = \frac{V_{stack}^2}{4R_{stack}} \tag{17}$$

If the power density is defined as power output per unit membrane area, the maximum power density P_{max} (W m^{-2}) is

then calculated as

$$P_{max} = \frac{V_{stack}^2}{4AR_{stack}} \quad (18)$$

where A is the membrane area (m^2).

If the loss of energy from pumping water through the system is considered, the net energy density (P_{net}) can be estimated using the following equations [66]:

$$P_{pump} = \Delta P_c Q_c + \Delta P_d Q_d \quad (19)$$

$$P_{net} = P_{max} - P_{pump} \quad (20)$$

where P_{pump} is the power density decrease due to hydrodynamic losses ($W\ m^{-2}$), ΔP_c and ΔP_d are pressure drops (Pa) over the concentrated and diluted compartments, respectively,. Q_c and Q_d are flow rates ($m^3\ s^{-1}$) in concentrated and diluted compartments, respectively.

P_{net} is a better indicator of the efficiency of the RED system because it takes both energy gain and energy loss into account. It should also be considered that the power output cannot be maintained at the maximum value in the real practice of the RED system because P_{max} is based on the largest concentration difference of the solutions on both sides at the beginning of the process. Inevitably, the concentration difference would decrease as well as the power output.

It should be noted that the gross power density reported in literature could be obtained from the theoretical calculation based on Eq. (17) or measured experimentally [13,18,26,50]. Generally, the experimental power density using the chronopotentiometry or the galvanostatic method is lower than the calculated value [26,30,67]. This problem of low power density can escalate because if the electrochemical property of the entire stack is not ideal, effects such as concentration polarization can be severely detrimental.

In addition, there are ions other than sodium (Na^+) and chloride (Cl^-) ions in seawater and river water. Multivalent ions, such as magnesium (Mg^{2+}) and sulfate (SO_4^{2-}) ions, also exist at a relatively lower concentration than salt. Post et al. [68] identified the potential detrimental effects of multivalent ions. A multivalent ion concentration of 0.05 M in a concentrated solution and 2 mM in a diluted solution (base NaCl solution of 0.45 M and 3 mM, respectively) decreases stack voltage and increases stack resistance [68]. Their effects may also be important to the total efficiency of RED power generation. Hong et al. [69,70] reported the modeling result to be a 15–43% decrease of power density in a system using simulated saline water as electrolytes flowing through RED stacks [69,70]. Vermaas et al. [71] also conducted experiments on RED stacks and used a mixture of 10% $MgSO_4$ and 90% NaCl (molar ratio). The resulting power density decreased by 29–50%, depending on the different IEM pairs tested [71].

3. Potential IEMs for RED

The need for the development of proper ion exchange membranes has been stressed in many reported studies on RED. Despite that, most efforts have been focused on system efficiency in regard to stack (e.g., cell configuration, spacers, and electrodes), design, and operation but not on membrane development for power performance. In most RED studies, commercially available IEMs were used (Tables 2 and 3), but such membranes were designed specifically for other applications, such as electrodialysis, diffusion dialysis, and electrodeionization. These other applications normally require different physical and electrochemical characteristics of membranes; hence, most currently available commercial membranes cannot meet RED membranes' required conditions. Although some commercial membranes contain a few desired properties needed for RED (e.g., high permselectivity), their high prices are still a significant hindrance in the smooth transition to commercialization of RED power generation.

Recently, some research efforts have been reported on designing tailor-made membranes for RED application. Depending on their design purpose (e.g., cation-/anion-exchangeable, monovalent-selective, and microstructured), proper structural modifications or chemical reactions were tested using different preparation methods and materials. In the next section, RED membrane preparations, potential membrane materials, and currently available RED IEMs (i.e., commercial and tailor-made) are discussed in detail to provide an overview on the current status of RED membranes and an insight into the development of cost-competitive and optimized membranes for RED application.

3.1. Preparation of cation exchange membranes (CEMs)

Ion exchange membranes (IEMs) determine the energy efficiency of a RED system, making membranes one of the most important components. IEMs contain negatively or positively charged groups, which are attached to the membrane backbone and discriminate between cations and anions. CEMs allow cations and exclude anions, and AEMs allow anions and exclude cations. In general, fewer steps are required to manufacture CEMs than AEMs [17,72,73]. For cation exchange materials, fixed ionic groups can be appended by acidic functional groups to give cation character to the membrane. The most common acidic functional groups are carboxylic and sulfonic groups, but phosphonic acid and phosphoric acid groups are also being investigated. The carboxylation process often involves the radiation grafting of either acrylic acid or methacrylic acids onto polymer films [74–76]. Carboxylic groups can be introduced by radiation-induced grafting of epoxy acrylate monomers followed by the subsequent conversion of an epoxy group to a carboxylic group by a ring opening reaction [77]. Sulfonation is another common chemical modification of base polymers for various membrane processes such as water filtration, diffusion dialysis, electrodialysis, and water cleavage [78]. The sulfonation process is an electrophilic substitution that normally takes place on the aromatic ring to increase the desired charge density and the hydrophilicity of the polymer matrix. By enhancing the ionic charge transfer, this modification facilitates good electrical conductivity [79]. Typical sulfonating agents, such as sulfuric acid or chlorosulfonic acid, are often used for this treatment.

Of the existing polymeric materials for manufacturing CEMs, the perfluorinated or partially fluorinated materials are most frequently used in commercial applications. For example, Nafion® is the most commonly used perfluorosulfonic membrane in fuel cell technology. Although the Nafion® membrane has a high water selectivity and ion exchange capacity, it often presents poor conductivity. Moreover, adverse safety concerns and its high cost prevent its widespread application. The high cost stems from the fluorochemistry involved in the synthesis of perfluorosulfonic materials. Thus, omitting the fluorinate species in the polymer matrix (i.e., non-fluorinated) can significantly decrease the cost of manufacturing IEMs. Consequently, non-fluorinated hydrocarbons are often considered to be an alternative material [80]. Moreover, as for membrane performance, fluorinated materials show good thermal and chemical stability and mechanical properties; however, for the RED process, the thermal and chemical stability and mechanical properties of IEMs are not very crucial. Thus, the use of non-fluorinated hydrocarbon materials for the production of IEMs may be a promising option to lower the cost of the membranes and to retain the high performance of the fluorinated materials. As mentioned previously, the functionalization of non-fluorinated polymers can be readily used for ion exchange in the RED system. For example, Guler et al. [30] investigated the bulk membrane properties of tailor-made membranes. For the synthesis of tailor-

Table 1
Existing nanocomposite membranes of various applications.

Nanomaterial	Organic material	Swelling degree (%)	IEC (meq g^{-1})	Conductivity/resistance	Applications	Refs.
Al_2O_3	PVA	–	–	0.2–0.4 Ω cm^2	Quaternized composite membrane for alkaline DMFC	[94]
CeO_2	Nafion	17–22	–	0.018 S cm^{-1}	Chemically durable proton exchange membrane for fuel cells	[108]
$Cu_3(PO_4)_2$ $Ni_3(PO_4)_2$	PVC	–	–	–	Electrochemical evaluation of two composite IEMs	[100]
Fe_2O_3	Nafion	22.9–40.7	–	–	High proton conductivity composite membrane for DMFC	[109]
Fe_2O_3	PPO	20–26	0.87–1.4	0.87–2.05 Ω cm^2	Salinity gradient power generation using RED	[12]
Fe_2NiO_4	PVC	17–23	1.5–1.6	9.1–12.8 Ω cm^2	Performance evaluation of heterogeneous CEM	[103]
MWCNT	PVA	38.2–284.0	0.7–2.25	–	Crosslinked nanocomposite membrane for DMFC	[95]
SiO_2	PPO	45.2–325.9	1.3–2.0	0.001–0.0085 S cm^{-1}	AEM for alkaline fuel cells: effect of heat treatment	[98]
SiO_2	PVA	–	1.0–1.26	–	Electrochemical characterization of AEM	[110]
SiO_2	PPO	20–27	0.7–1.0	–	Fuel cell application	[111]
SiO_2	PVA	32–54	0.6–1.2	0.004–0.014 S cm^{-1}	Thermally stable CEMs for fuel cell and chlor-alkali application	[112]
SiO_2	PVA/PPO	100–475	0.5–1.35	–	Double organic phases for diffusion dialysis (alkali recovery)	[93]
SiO_2	PVDF	10–26.2	1.25–2.0	0.0026–0.0041 S cm^{-1}	Electrochemical characterization of CEM	[107]
SiO_2	Nafion	3–9	–	–	Proton conducting membrane for DMFC	[113]
SiO_2	Nafion	20–35	–	–	Investigation of composite membrane for PEMFC	[114]
SiO_2	PES	9.7–14.3	0.74–1.1	0.00007–0.00024 S cm^{-1}	Electrodialysis IEM for desalination	[115]
SiO_2	PPEK	28–70	–	–	Proton exchange membrane for DMFC	[116]
SiO_2	PAES	26–37.5	–	0.08–0.13 S cm^{-1}	Fuel cell application	[117]
SiO_2	PS	–	0.48–1.3	0.00007–0.0003 S cm^{-1}	Performance evaluation: proton and methanol transport	[118]
SiH_4	PEO	127–203	0.4–0.99	–	Thermally stable negatively charged NF membrane	[119]
TiO_2	PES	–	–	–	UV-irradiated TiO_2 for modification of UF membrane	[120]
TiO_2	PES	–	–	–	Performance evaluation of PES composite membrane	[121]
TiO_2	Nafion	30–36.5	–	0.0705–0.0947 S cm^{-1}	Solid superacid composite membrane for DMFC	[122]
TiO_2	Nafion	–	–	–	Electrochemical performance for DMFC	[123]
TiO_2	PVA	20–130	–	–	Pervaporation separation of water–isopropanol mixture	[124]
TiO_2	PVDF	–	–	–	Anti-fouling performance and water treatment	[125]
TiO_2	PES/PVA	40–110	–	–	Flux and salt rejection of NF membrane	[126]
ZrO_2	Nafion	–	–	–	Asymmetric hybrid membrane for gas permeability	[127]
ZrO_2	Nafion	21–27	0.9–1.13	–	Conductive composite membrane for PEMFC	[128]
ZrO_2	Nafion	–	–	0.13–0.15 Ω cm^2	Solid polymer electrolyte electrolyzer application	[106]
ZrO_2	PVDF	–	–	–	Performance evaluation of UF membrane	[129]
ZrO_2	Nafion	20–30	0.84–0.92	–	Performance at high temperature/low humidity for PEMFC	[130]
ZrO_2	Nafion	–	–	–	Proton conductivity for high temperature DMFC	[131]

PPO: poly (2,6-dimethyl-1,4-phenylene oxide); PVA: polyvinyl alcohol; PVDF: polyvinylidene fluoride; PVC: polyvinyl chloride; PES: polyethersulfone; PPEK: poly (phthalazinone ether ketone); PAES: poly(arylene ether sulfone); PS: polystyrene; PEO: polyethylene oxide; MWNT: multi-walled carbon nanotube; PEM: polymer electrolyte membrane; PEMFC: proton exchange membrane fuel cell; DMFC: direct methanol fuel cell; NF: nanofiltration; UF: ultrafiltration.

made CEMs, a non-fluorinated thermoplastic polymer, sulfonated polyetheretherketone (SPEEK), was used. Tailor-made CEMs under different sulfonation degrees performed well in the RED stack, producing excellent electrochemical properties and high power output.

3.2. Preparation of anion exchange membranes (AEMs)

A number of studies and various approaches have proposed methods for preparing AEMs to combine with the desired cationic moieties. The cationic moieties in the membrane can be introduced either prior to dissolving a polymer for casting the membrane or after dissolving a polymer for casting the membrane. Typical chemical modifications of polymer films for the preparation of AEMs usually consist of two steps: a chloromethylation followed by quaternary amination. Prior to the quaternary ammonium functionalization reaction, the polymer film can be modified by direct or indirect grafting of vinyl monomers (e.g., sodium p-styrene sulfonate) to introduce ionic characteristics. The commonly used chloromethyl methyl ether during the chloromethylation has some drawbacks; it is a highly toxic and carcinogenic reagent with a potential risk to human health, and it is difficult to control the position and the quantity of the methyl groups [81]. Several studies have avoided the use of chloromethyl methyl ether in preparing AEMs. The use of *N*-bromosuccinimide (NBS) as the halomethylation agent for bromomethylation [82] or paraformaldehyde and the use of concentrated hydrochloric acid as the chloromethylating agent for chloromethylation [83] were considered for use with methyl-containing polymers (e.g., polyepichlorohydrin (PECH), polysulfone, and polyphenylene) to be a safer and more controllable treatment. Direct grafting copolymerization of pyridine or vinylbenzylchloride onto polymer films or copolymerization with other monomers could also serve as alternative routes to prepare AEM with a subsequent quaternary amination reaction [84,85].

The quaternary ammonium functionalization groups can be grafted as charge carriers onto the polymer backbone by using either strongly basic (e.g., tertiary ammonium) or weakly basic (e.g., primary, secondary, or tertiary amine) groups. The cast membranes are often immersed into an appropriate functionalizing agent for quaternization; however, the quaternization of the dried (cast) membranes limits the degree of desired functionality [81]. Zhao et al. [81] used a more quantitative method of quaternization to prepare the alkaline AEMs. Instead of quaternizing the membranes in the solid state, the homogeneous amination method was used by adjusting the addition of trimethylamine (TMA), which is an aminating agent. The homogeneous amination method can achieve good results in a more controllable and selective fashion. This quaternization method has been optimized to work faster and easier in controlling the degree of functionalization, resulting in an improved selectivity and ion exchange capacity (IEC) of the membrane.

In order to obtain the required mechanical and chemical stability of a functionalized polymer, the crosslinking reaction is critical; however, the use of excess crosslinking often decreases the ionic conductivity of the membranes [86]. Increasing the degree of crosslinking narrows the path of ion transport in the membrane, which can lead to poor ionic conductivities. Thus, the

Table 2
Properties of commercially available and custom-made IEMs.

Membrane product	IEC (meq g_{dry}^{-1})	Permselectivity (%)[a]	Resistance (Ω cm^2)[b]	Swelling degree (%)	Thickness (μm)	Ionogenic groups	Refs.
Cation ion exchange membranes							
Homogeneous							
Fumasep® FKD	1.14	89.5	2.14	29	113	$-SO_3^{2-}$	[37]
Fumasep® FKS	1.54	94.2	1.5	13.5	40	–	[30]
Qianqiu CEM	1.21	82.0	1.97	33.0	205	–	[30]
Neosepta® CMX	1.62	99.0	2.91	18	164	$-SO_3^{2-}$	[26]
Neosepta® CMX	1.5–1.8	97	1.8–3.8	25–30	140–200	$-SO_3^{2-}$	[16]
Selemion® CMV	2.0–2.4	95.0–98.8	2.3–2.9	20–25	101–150	$-SO_3^{2-}$	[16,26]
0.7 wt% Fe_2O_3–SO_4^{2-} sPPO	1.40	87.7	0.97	26	100	$-SO_3^{2-}$	[12]
SPEEK 40	1.23	95.3	2.05	23	53	$-SO_3^{2-}$	[30]
SPEEK 65	1.76	89.1	1.22	35.6	72	$-SO_3^{2-}$	[30]
JJC-82		99.6	3.1				[8]
Heterogeneous							
Ralex® CMH-PES	2.34	94.7	11.33	31	764	$-SO_3^{2-}$	[26]
Anion exchange membranes							
Homogeneous							
Fumasep® FAD	1.42	86.0	0.89	34	74	–	[26,30]
Neosepta® ACS	1.4–2.0	–	2.0–2.5	20–30	150–200	$-N(CH_3)_3^+$	[134]
Neosepta® AMV	1.78–1.9	87.3	3.15	17.0	120–124	–	[16,30]
Neosepta® AMX	1.4–1.7	90.7	2.0–3.5	25–30	120–180	$-N(CH_3)_3^+$	[134,135]
Selemion® ASV		97	3.7		120		[c]
Fumasep® FAS	1.12	89.4	1.03	8.0	33	–	[30]
Qianqiu AEM	1.33	86.3	2.85	35.0	294	–	[30]
PECH A	1.31	90.3	2.05	32.2	77	–NR3+	[13]
PECH B-1	1.68	86.5	0.82	49	33	–NR3+	[13]
PECH B-2	1.68	87.2	0.94	49	77	–NR3+	[13]
PECH B-3	1.68	87.0	1.32	49.1	130	–NR3+	[13]
PECH C	1.88	79.2	1.14	53.5	77	–NR3+	[13]
Heterogeneous							
JJA-72		99	3.0				[8]
Ralex® AMH-PES	1.97	89.3	7.66	56	714	–	[26]

[a] Measured over the membrane between a 0.5 M and a 0.1 M solution.
[b] Measured in 0.5 M NaCl solution at 25 °C.
[c] From manufacturer.

addition of crosslinking should be optimized depending on the polymers and applications. In addition, the application of tertiary diamines biquaternization should also be considered. Komkova et al. [79] treated the AEM casting solution with diamines to introduce positively charged groups into the polymer (i.e., mono-quaternization) and to carry out a crosslinking reaction (i.e., bi-quaternization); however, it is important to note that the type and the amount of the quaternization agent (or crosslinker) applied in the AEM preparation should be optimized to obtain desirable electrochemical properties specific to RED application. In general, an excess of diamines is preferable with a short chain length of alkyl groups to achieve high permselectivity and low membrane resistance [87], but an excess of diamines with a long aliphatic chain of the alkyl groups has exhibited a decrease in IEC and permselectivity and an increase in membrane resistance [79]. Thus, the quaternization and the crosslinking reaction in the case of a long chain of alkyl groups (i.e., bonded to amine nitrogen) requires less diamines to obtain AEMs with a low membrane resistance and a high permselectivity, which is more favorable to the RED system.

3.3. Potential membrane materials

In IEM applications, membrane characteristics are mainly dependent on the amount of charged species groups and their distribution within the membranes [17]. Different properties of commercially available IEMs were investigated in order to evaluate their potential performance under RED conditions by Dlugolecki et al. [26]. In this study, membranes were selected based on their low resistance and high selectivity. In general, membranes used in electrochemical systems, such as RED, are characterized based on their IEC, permselectivity, electrical resistance, charge density, and swelling degree [26,30]. These electrochemical properties are directly affected by their structure (thickness and porosity), the preparation procedure (phase inversion and functionalization), and the chemical composition of the membranes. An evaluation of the basic properties of the membranes and their interconnectedness is necessary to optimize the performance of IEMs for efficient power generation. At the same time, appropriate membrane materials should also be used to lower the cost of membrane manufacturing. An ongoing challenge in this field is to develop cost-competitive membranes with the desired properties for RED applications. The cost of RED membrane materials is expected to be reduced as the energy conversion system matures.

As previously mentioned, the ideal RED IEMs can be selected based on their electrochemical properties, which are mainly determined by the concentration of mobile ions in the membranes and the mobility of the ions in the membrane phase. Polymer-based IEMs are expected to possess both chemical stability and excellent conductivity when the polymers are incorporated into charged groups. Although, in theory, all IEMs can be used for RED, current commercially available IEMs are not ideal for RED application because they often lack the abilities to enhance power output. The desired membranes should not only possess low resistance and high selectivity but should also be easy to prepare and cost competitive. Therefore, the desired or competitive polymer

Table 3
Power density reported in the literature.

Manufacture/tailor made	CEM	AEM	Spacer type/thickness	Unit membrane area	Cell no.	Linear flow velocity	Concentration gradient	Gross power density (W/m^2)[a]	Refs.
–	Polyethylene mixed with crosslinked polystyrene resins		Nonconductive spacer 1000 μm	8 cm^2	47	–	Tap water/ 0.5 M NaCl	0.20 (39 °C)	[2]
Ionics	61CZL	103QZL	Turbulence promoter 1000 μm	232 cm^2	30	15 cm s^{-1}	0.0259/0.57 M NaCl		[136]
Rhone-Poulenc	CRP	ARP	Nonconductive 3000 μm	40 cm^2	5	–	0.017/5.03 M NaCl	0.41	[137]
Asahi	CMV	AMV	Nonconductive 3000 μm	40 cm^2	5		0.017/5.03 M NaCl	0.4	[137]
MEGA	CMH-PES	AMH-PES	Nonconductive 200 μm	100 cm^2	5	1.7 cm s^{-1}	0.017/0.513 M NaCl	0.6	[30]
MEGA	CMH-PES	AMH-PES	Nonconductive 250 μm	100 cm^2	5	17 cm s^{-1}	0.017/0.508 M NaCl	0.65	[61]
Modified commercial polyethylene	JJC-82	JJA-72	Polyethylene spacer 550 μm	100 cm^2	30	0.21 cm s^{-1}	0.008/0.561 M NaCl	0.41	[8]
Modified Commercial Polyethylene	JJC-82	JJA-72	Polyethylene spacer 550 μm	100 cm^2	30	0.21 cm s^{-1}	0.017/0.556 M NaCl	0.388	[8]
Modified commercial polyethylene	JJC-82	JJA-72	Polyethylene spacer 550 μm	100 cm^2	30	0.21 cm s^{-1}	0.55/5.32 M NaCl	0.573	[8]
ACIPLEX	K-502	A-201	1 mm spacer for dilute; 10 mm spacer for salt	80 cm^2	29	1.9 cm s^{-1} for dilute; 0.075 cm s^{-1} for saline[b]	0.0017/0.598 M NaCl	0.26	[55]
Fumatech	FKS	FAS	Nonconductive 200 μm	100 cm^2	5	1.7 cm s^{-1}	0.017/0.513 M NaCl	1.11	[30]
Fumatech	FKS	FAS	Nonconductive 100 μm	100 cm^2	5	4 cm s^{-1}[b]	0.017/0.507 M NaCl	2.2	[18]
Custom-made	SPEEK40	PECH B2	Nonconductive 200 μm	100 cm^2	5	1.7 cm s^{-1}	0.017/0.513 M NaCl	1.18	[30]
Custom-made	SPEEK 65	PECH B2	Nonconductive 200 μm	100 cm^2	5	1.7 cm s^{-1}	0.017/0.513 M NaCl	1.28	[30]
Tokuyama/custom-made	CMX	PECH B3	Nonconductive 200 μm	100 cm^2	5	1.7 cm s^{-1}	0.017/0.513 M NaCl	1.07	[30]
Custom-made/ Tokuyama	SPEEK40	AMX	Nonconductive 200 μm	100 cm^2	5	1.7 cm s^{-1}	0.017/0.513 M NaCl	0.98	[30]
Tokuyama/custom-made	CMX	PECH B2	Nonconductive 200 μm	100 cm^2	5	1.7 cm s^{-1}	0.017/0.513 M NaCl	1.18	[30]
Qianqiu	Qianqiu CEM	Qianqiu AEM	Nonconductive 200 μm	100 cm^2	5	1.7 cm s^{-1}	0.017/0.513 M NaCl	0.83	[30]
Custom-made/ Tokuyama	SPEEK65	AMX	Nonconductive 200 μm	100 cm^2	5	1.7 cm s^{-1}	0.017/0.513 M NaCl	1.1	[30]
Tokuyama/Custom-made	CMX	PECH B1	Nonconductive 200 μm	100 cm^2	5	1.7 cm s^{-1}	0.017/0.513 M NaCl	1.27	[30]
Tokuyama/custom-made	CMX	PECH A	Nonconductive 200 μm	100 cm^2	5	1.7 cm s^{-1}	0.017/0.513 M NaCl	1.08	[30]
Tokuyama/custom-made	CMX	PECH C	Nonconductive 200 μm	100 cm^2	5	1.7 cm s^{-1}	0.017/0.513 M NaCl	1.15	[30]
Asahi Glass	CMV	AMV	Nonconductive 200 μm	100 cm^2	5	1.7 cm s^{-1}	0.017/0.513 M NaCl	1.13	[30]
Tokuyama	CMX	AMX	Nonconductive 200 μm	100 cm^2	5	1.7 cm s^{-1}	0.017/0.513 M NaCl	1.07	[30]
Fumatech	FKD	FAD	Nonconductive 200 μm	100 cm^2	5	1.7 cm s^{-1}	0.017/0.513 M NaCl	1.19	[30]
Fumatech	FKD	FAD	Nonconductive 200 μm	100 cm^2	25	1.16 cm s^{-1}[b]	0.017/0.51 M NaCl	1.17	[67]

Fumatech	FKD	FAD	Nonconductive spacer 200 μm	100 cm^2	50	6.7 cm s^{-1}[b]	0.017/0.513 M NaCl	0.93	[67]
Fumatech	FKD	FAD	Nonconductive 200 μm	100 cm^2	50	0.58 cm s^{-1}[b]	0.017/0.51 M NaCl	0.95	[47]
Custom-made	Profiled CMH-PES	Profiled AMH-PES	Profiled IEMs serves as spacers 230 μm	100 cm^2	6	21 cm s^{-1}	0.017/0.508 M NaCl	1.0	[61]
Tokuyama/custom-made	CMX	PECH (Pillar structure)	Nonconductive in concentrated compartment 100 μm; AEM serves as spacers in dilute compartment 100 μm	100 cm^2	2	6.7 cm s^{-1}[b]	0.017/0.507 M NaCl	1.3	[14]
Tokuyama/custom-made	CMX	PECH (Wave structure)	Nonconductive in concentrated compartment 100 μm; AEM serves as spacers 100 um	100 cm^2	2	6.7 cm s^{-1}[b]	0.017/0.507 M NaCl	1.3	[14]
Tokuyama/custom-made	CMX	PECH (Ridge structure)	Nonconductive in concentrated compartment 100 μm; AEM serves as spacers 100 um	100 cm^2	2	6.7 cm s^{-1}[b]	0.017/0.507 M NaCl	1.1	[14]
Tokuyama/custom-made	CMX	PECH (Flat)	Nonconductive 100 μm	100 cm^2	2	6.7 cm s^{-1}[b]	0.017/0.507 M NaCl	0.9	[14]
Tokuyama	CMX	AMX	Nonconductive 190 μm	42 cm^2	10	0.54 cm s^{-1}	0.0096/0.605 M NaCl	0.46	[138]
Tokuyama	CMX	AMX	Ion conductive spacer 320 μm	100 cm^2	3	0.83 cm s^{-1}	0.017/0.5 M NaCl	0.8	[139]
Tokuyama	CMX	AMX	Nonconductive spacer 320 μm	100 cm^2	3	0.83 cm s^{-1}	0.017/0.5 M NaCl	0.27	[139]
Neosepta	CMX	AMX	Nonconductive 200 μm	100 cm^2	25	1.16 cm s^{-1}[b]	0.017/0.51 M NaCl	0.65	[67]
Asahi Glass	CMV	AMV	Nonconductive 200 μm	100 cm^2	25	1.16 cm s^{-1}[b]	0.017/0.51 M NaCl	1.18	[67]
Neosepta	CMS	ACS	Nonconductive 200 μm	100 cm^2	25	1.16 cm s^{-1}[b]	0.017/0.51 M NaCl	0.60	[67]
Qianqiu	Qianqiu CEM	Qianqiu AEM	Nonconductive 200 μm	75 cm^2	25	2.7 cm s^{-1}	0.017/0.51 M NaCl	0.82	[66]
Qianqiu	Qianqiu CEM	Qianqiu AEM	Nonconductive 200 μm	100 cm^2	25	1.16 cm s^{-1}[b]	0.017/0.51 M NaCl	1.05	[67]
Custom-made/ Selemion	0.7 wt% Fe_2O_3–SO_4^{2-} sPPO	ASV	Nonconductive 250 μm	36 cm^2	3	6.7 cm s^{-1}	0.017/0.51 M NaCl	1.3	[12]

[a] Listed the highest gross power density achieved only.
[b] Calculated based on information provided.

materials for RED IEM preparation must have several characteristics. First, the polymers should be functionalized easily, making it possible to bind the main chain of the polymer with charged groups. Second, the polymer preparation process should be simple and manageable, meaning they can dissolve at room temperature and will not release toxic substances during membrane preparation. Third, the polymeric materials should be affordable based on the cost of RED membranes and systems in large scale applications according to economies of scale. Three exemplary and most frequently used low-cost IEM materials (i.e., PVA, PPO, and PVC) are discussed in the following sections.

3.3.1. Polyvinyl alcohol (PVA)

Polyvinyl alcohol (PVA) is a polyhydroxy polymer that has received increasing attention because of its high hydrophilicity, good chemical-resistance, good membrane-formation, and low cost in IEM applications [88]. The highly dense reactive chemical functions of PVA make this polymer more favorable for crosslinking through irradiation, chemical, or thermal treatments [75]. The commercial production of PVA is based on the hydrolysis of an acetate by ester interchange with methanol in the presence of anhydrous sodium methylate or aqueous sodium hydroxide. PVA is an odorless, non-toxic, and water-soluble polymer that readily reacts with different crosslinking agents to form a gel (Fig. 3(a)). It is also biocompatible and biodegradable, which allows it to be widely used in various applications, such as in the medical, cosmetic, and packaging industries.

However, the absence of charged ionic groups in the pure PVA polymer matrix results in poor conductivity. For PVA to possess reasonable ionic conductivity, chemical or physical modification is required to allow entrance of charged ionic species into the PVA membrane. PVA-based membranes can be modified by crosslinking, blending, and acid or base treatments. Generally, the desired conductivity of the PVA membrane can be obtained through an electrophilic substitution process using either sulfonating agents for CEMs or aminating agents for AEMs. For example, Rhim et al. [89] introduced negatively charged groups ($-SO_3H$) to PVA using a crosslinking agent, sulfosuccinic acid (SSA), for fuel cell applications. The crosslinked PVA membranes with sulfonic groups exhibited improved conductivity at a range of 10^{-3}–10^{-2} S cm^{-1}. The IEC was also enhanced significantly as the applied SSA amount increased, reaching 2.24 meq g^{-1} with 30 wt% SSA [89].

PVA can also be crosslinked with a quaternized cationic polymer using a combined heat and chemical treatment. Zhang et al. [90] used a simple blending technique to crosslink PVA with PDDA (poly (diallyldimethylammonium chloride)) by applying glutaraldehyde (GA). This PVA-based AEM simplified the preparation process by blending directly with the cationic polymer, PDDA, which contains the cyclic quaternary ammonium structure. Thus, PVA/PDDA should be able to use anions as charge carriers. In addition, the heat treatment and the use of GA for crosslinking enhanced the thermal and mechanical stability of the membrane. Synthesized PVA/PDDA membranes exhibited high conductivity and yielded a power density comparable to commercially available membranes for alkaline fuel cells, suggesting that PVA membranes in combination with other cationic polymers (e.g., PDDA) could be a potential approach to preparing AEMs for RED application.

Inorganic filler particles provide extra functional groups in the membrane, which helps with ion migration and, therefore, improve membrane conductivity [12,91]. In addition to introducing functional groups to the membrane backbone, inorganic fillers are often used on the polymer electrolyte membrane in the form of nanoparticles. Blending filler materials into the PVA polymer can be a promising approach to enhance the physical and electrochemical properties of the membranes. There are several inorganic fillers used to mix with PVA based membranes, including Al_2O_3, SiO_2, TiO_2, and MWNT [92–95]. Designing a nanocomposite structure for RED membranes is further discussed in the following section.

3.3.2. Poly (2,6-dimethyl-1,4-phenylene oxide) (PPO)

Poly (2,6-dimethyl-1,4-phenylene oxide) (PPO) is a prospective RED membrane material because of its low cost, high film-forming properties, good mechanical, thermal, and chemical stability, low-moisture uptake, and high glass transition temperature [96]. The basic form of PPO consists of an aromatic ring, two methyl groups, and a phenol group (Fig. 3(b)). The simple structure of PPO allows for various structural modifications. For example, the benzene rings and the methyl groups of the PPO chains can be functionalized through electrophilic or radical substitutions, capping, and coupling. These functionalizations introduce desired charged groups into the PPO polymer matrix, which makes the polymer more adequate for ion exchange. In the case of CEMs, sulfonated PPO (sPPO) is often prepared by functionalizing the aromatic rings of the polymer chains with charged groups, typically from sulfonic acid. sPPOs have been widely used in various industrial applications due to their excellent electrochemical characteristics [75,97].

In addition to pure PPO-based membranes, PPO-based organic–inorganic hybrid IEMs have also been well-studied for enhanced thermal stability and mechanical strength. It is reported that SiO_2 was blended into PPO through a sol–gel process of the polymer precursors PPO–Si $(OCH_3)_3$ using tetraethoxysilane (TEOS) as the Si source. Also, this membrane was found to possess enhanced hydroxyl (OH^-) conductivity, which is useful for alkaline fuel cells. The membranes exhibited higher swelling-resistant properties, and the hydroxyl ion (OH^-) conductivity values were comparable to previously reported fluoropolymer-containing membranes (0.012–0.035 S cm^{-1} in the temperature range 30–90 °C). In addition, if these membranes were heat-treated at 120–140 °C for different times during its preparation, the physicochemical properties of the membranes, including IEC, hydrophilicity, OH^- conductivity, and tensile strength, could be easily controlled by adjusting the heating temperature and time [98].

In addition to inorganic particle-blended PPO membranes, PPO can also be blended with organic materials. The sPPO and PVA were crosslinked by double crosslinking agents, monophenyl triethoxysilane (EPh) and tetraethoxysilane (TEOS), through the sol–gel process [93]. Wu et al. [77] prepared the cation exchange hybrid membranes for application in a diffusion dialysis (DD) process. The sPPO membranes often perform poorly in aqueous separation processes (e.g., DD process) and easily erode in organic solvents. Thus, sPPO-based IEMs can be modified by mixing them with other polymers that are potentially more stable in organic solvents with a high membrane forming ability (e.g., PVA). This type of PPO-based membrane formation is reported to enhance IEC by providing thermal and mechanical stability, resistivity to organic solvents, and ion transport characteristics (from the use of silanes as crosslinkers) [93].

3.3.3. Polyvinylchloride (PVC)

Polyvinylchloride (PVC) is another flexible polymer with a good thermal, biological, and chemical resistance. Its low price makes the

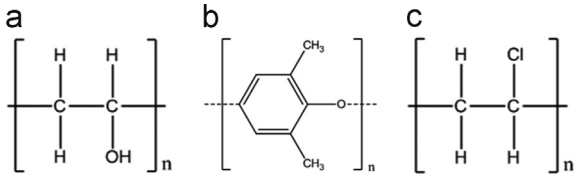

Fig. 3. Basic chemical structure of (a) polyvinyl alcohol, (b) poly (2,6-dimethyl-1,4-phenylene oxide), and (c) polyvinylchloride.

material more attractive in the fabrication of membranes (Fig. 3(c)) [99]. PVC has been used in various industrial applications, such as in chemical processes, biotechnology, and water treatment [100,101]. Hosseini et al.#[10] used PVC as a base membrane blended with cellulose acetate (CA) to prepare the heterogeneous CEMs for the electrodialysis process. The effect of the blended ratio of polymers (PVC to CA) on the physicochemical characteristics of the membranes showed that the IEC was enhanced with the increase of CA ratio loading. PVC-based strong acidic CEMs are also prepared by using different types of binders (i.e., suspension and emulsion PVCs) and plasticizers [102]. The water content of the membranes was 30–40%, and the IECs varied between 1.2 and 2.8 meq g^{-1}. The highest IEC was obtained when the suspension polymerized PVC (S-PVC) was coupled with an ionic liquid (IL) or dioctyl phthalate (DOP). Both DOP-based and IL-based membranes had comparable physicochemical and morphological properties, but IL-based membranes showed better electrochemical properties than those of DOP-based membranes. The use of the suspension polymer binder with an adequate plasticizer (i.e., IL) could be an effective approach to preparing RED IEMs once the high conductivity of the membrane material is ensured. PVC can also be used in preparing AEMs via plasma grafting, quaternization, and alkalization [101]. Hu et al. [101] synthesized a plasma-grafted AEM using PVC powders; this process showed promising electrochemical performance of IEC and open circuit voltage (OCV), which increases the attractiveness of PVC as a potential RED membrane material.

In recent years, inorganic nanoparticles gained increased attention as a filler material of polymeric membranes due to the effective role in membrane performance. For example, Hosseini et al. [103] used iron-nickel oxide (Fe_2NiO_4) nanoparticles blended with PVC/styrene-butadiene-rubber (SBR) to prepare heterogeneous CEM through a solution casting technique. This study showed that the IEC, charge density, and permselectivity of membranes improved with the increase of nanoparticle concentration until reaching a certain level of loadings. In addition, Arsalan et al. [100] prepared two PVC-based composite IEMs using the sol–gel method: $Cu_3(PO_4)_2$ and polystyrene supported $Ni_3(PO_4)_2$, respectively. Both composite membranes showed high stability due to its favorable polymer interaction and high cation selectivities.

3.4. RED membranes in progress

The successful implementation of RED as a feasible sustainable technology for power generation depends on optimizing membrane characteristics and minimizing cost. Currently, commercially available IEMs are not ideal for RED because they lack enhancement in certain membrane properties necessary for this application. Various preparation methods and materials for RED membrane synthesis have been explored. The synthesis of custom-made RED membranes in recent years has improved membrane properties, leading to higher power density yields. One such experiment synthesized an AEM using polyepichlorohydrin (PECH) for an elastopolymer matrix, which eliminated the need for the chloromethylation reaction since PECH has inherent chloromethyl groups [13]. 1,4-diazabicyclo-[2.2.2]octane (DABCO) was applied for crosslinking and the introduction of positively charged ionic groups. To avoid brittleness in water due to the high swelling degree, the inert polymer polyacrylonitrile (PAN) was added. The resultant membranes fabricated with the controlled amount of PAN exhibited acceptable mechanical strength at a high swelling degree; however, the permselectivity of the membranes decreased, and the resistance showed no significant changes as the blend ratio of PECH and PAN (m_{PECH}/m_{PAN}) increased. This was attributed to the increasing degree of swelling with the increasing amount of functional chloromethyl groups in the active polymer (i.e., PECH). The use of DABCO also clearly indicated the existence of optimal concentration, and the amount completed the amination of all chloromethyl groups of the polymer. Thus, the IEC and the permselectivity showed an increase until a peak of 4.2 was reached at the diamine ratio (the molar ratio of the amine component (DABCO) over the chloromethyl groups in PECH). These custom-made changes improved the power density when compared with commercially available AEMs. The best performer of the PECH membranes at a power density of 1.2 W m^{-2} was at an excess diamine ratio of 4.2 and a blend ratio (m_{PECH}/m_{PAN}) of 0.333. Its properties included low membrane resistance and high permselectivity.

Trials with custom-made membranes using cation-exchanging sulfonated polyetheretherketone (SPEEK) and anion-exchanging PECH in a RED stack decreased membrane resistance and, therefore, increased the gross power density versus the commercially available membrane stack [30]. This study prepared the PECH AEMs using a solvent evaporation method. Sulfonated SPEEK (65% and 40% sulfonation degree) CEMs were dissolved in 10 and 20 wt % N-methyl-2-pyrrolidon (NMP), cast with an average thickness of 70 μm for SPEEK65 membranes and 55 μm for SPEEK40 membranes, and dried. The PECH AEMs and SPEEK CEMs were characterized by electrochemical and physical properties and then tested in a complete RED stack. This study showed that the thickness of the membrane has no significant effect on IEC, SD, and permselectivity when the membranes are formed with the same chemical composition; however, a decrease in the thickness (~33 μm) played a crucial role because it promoted faster ion transfer through the membrane, leading to a lower area resistance. This work provides evidence that low membrane resistance contributes significantly to optimizing the power density of RED membrane stacks, whereas high permselectivity only has a limited effect. Compared with RED stacks made with commercially available membranes, the custom-made RED stack exhibited the highest gross power density (1.3 W m^{-2}).

RED performance can be limited by the presence of multivalent ions in natural waters where the process will take place [69,104]. Therefore, membranes with a high selectivity for monovalent ions are beneficial for RED applications. Guler et al. [104] were the first to prepare the tailor-made monovalent ion selective membranes. The standard AEMs were used with a coating on both sides to tailor the selectivity of monovalent ions for RED application [105]. The contents of the negatively-charged coating layer included 2-acryloylamido-2-methylprpanesulfonic acid (AMPS) as a polyanion with sulfonic groups and N,N-methylenebis (acrylamide) (MBA) as the crosslinking agent. To prepare the monovalent ion selective membranes, an in situ synthesis method was used on the reactive polymeric coating layer via UV irradiation on the membrane surface. This method preserved the bulk membrane structure, improved antifouling properties, such as hydrophilicity, and increased monovalent ion selectivity. The coated standard-grade commercial membrane performed similarly to commercially available monovalent-selective membranes in calculations of monovalent selectivity by bulk transport numbers, current-voltage, and limited current density. The performance measured in an RED stack using thick coated membranes (~110 μm and above) did not yield significantly higher gross power densities than that of the commercially available monovalent-selective membranes. Further research is needed with thinner membranes for perhaps a more significant improvement in power density.

A composite structure formed by introducing inorganic nanomaterial into an organic polymer matrix can also be a potential candidate for RED. Nanocomposite IEMs allow extra ion exchangeable functional groups into the structure, which is advantageous in enhancing the electrochemical characteristics of the membrane. Many membrane studies have focused on combining and deriving the unique features of various inorganic nanoparticles with those of organic materials, particularly in electrodialysis, fuel cell, and

water treatment applications (Table 1). Although the listed examples in Table 1 were not prepared for RED application, some of the characteristics reported are beneficial in facilitating the ionic current in an RED stack, which can be helpful for power generation. For example, the studies of Al_2O_3/PVA [94] and ZrO_2/Nafion [106] nanocomposite membranes showed some beneficial features that directly affect the power density, that is, a membrane area resistance of 0.2–0.4 $\Omega\,cm^2$ (Al_2O_3/PVA) and 0.13–0.15 $\Omega\,cm^2$ (ZrO_2/Nafion). Moreover, the combination of the multi-walled carbon nanotube/PVA [95] and SiO_2/PVDF [107] also exhibited a high degree of IEC with the controlled amount of nanomaterial used. Such studies support that both physico- and electrochemical properties (e.g., IEC, swelling degree, and resistance) of the resultant membranes were highly dependent on the nanoparticle amount applied in the polymer matrix.

Hong and Chen [12] reported the first work on nanocomposite CEMs applied in an RED stack for power generation. In this study, the functionalized iron (III) oxide (Fe_2O_3–SO_4^{2-}) was introduced into a sulfonated poly (2,6-dimethyl-1,4-phenylene oxide) (sPPO) polymer matrix under various concentration loadings. The electrochemical properties of the membranes were enhanced with increased Fe_2O_3–SO_4^{2-} loadings and were optimized at the range of 0.5–0.7 wt%. A relatively higher permselectivity (87.65%) and a lower area resistance (0.87 $\Omega\,cm^2$) were exhibited in the membrane containing 0.7 wt% Fe_2O_3–SO_4^{2-}. The highest gross power density obtained was 1.3 W m^{-2} in a RED stack, which exceeds the power output of the commercially available CSO (Selemion™, Japan) membrane. Structure modification is considered to an effective way to enhance ion transport while maintaining large surface-charged functional groups in the polymer matrix [28]. Hong and Chen [15] synthesized custom nanocomposite CEMs to make porous membrane structures of various thicknesses, aging (evaporation) time, and inorganic nanoparticle loadings. This engineered approach improved membrane conductivity thereby lowering resistance for higher electrical current flow throughout the RED system. The application of the pore-induced nanocomposite CEMs in an RED stack resulted in a power density of 1.4 W m^{-2} with the thinnest (i.e., 30 μm) membrane containing an optimal amount of Fe_2O_3–SO_4^{2-} (0.7 wt%). Customizing key structural properties of the membrane plays a significant role in ionic transport, resulting in higher RED power performance. Therefore, the structural optimization of the membrane in combination with the use of functionalized nanoparticles shows great potential as a feasible way to modify IEMs for an RED power generation process.

One other design strategy for RED membrane would create microstructures on the membrane surface. The concept of microstructured membranes allows the creation of channels for feed solutions, which could possibly integrate the role of membranes and spacers and, thus, eliminate the need for non-conductive spacers typically used in RED stacks. The applied water can be transferred into the formed compartment next to each ridge for migrating ions to the adjacent compartment. This concept was developed based on the idea of using a single ion-conducting body to avoid any possible blockage of ion transport. Such membranes can be prepared in various ways, but two techniques were reported for the fabrication of RED-specific membranes: hot-pressing [132] and the use of steel molds [14]. For the first time, Vermaas et al. [132] prepared the profiled RED membranes with two commercial heterogeneous membranes (Ralex CMH and AMH) using the hot-pressing (or hot-embossing) method. The prepared profiled membranes exhibited a significantly lower resistance and slightly higher power densities compared with those containing spacers. Due to the difficulties in preserving the microstructured form during the process of releasing the membrane film from the mold and its possible weakening effect on the membrane's electrochemical properties, the steel mold casting method was further investigated in different shapes of microstructures [14]. Three different membrane structures (ridges, waves, and pillars) performed well in a RED stack: the pillar-structured membranes achieved a 38% higher gross power density than that of the typical flat membrane-spacers coupled units. The study shows that the optimized structure geometry provided less hindrance to the water flow ensuring even distribution over the membrane surface and thus performed better in RED. This emphasizes that a highly conductive homogeneous membrane-spacer structure with more allowable flow space (flow direction-wise) is preferred. In addition, considering the fact that decreasing membrane thickness enhances ion transport through the membrane and thus allows for low membrane resistance, the thickness of these structured membranes needs to be optimized. Controlled thickness of microstructured membranes (i.e., both thickness of the membrane base and the microstructure) should be strong enough to provide the required flow channel without spacers as well as avoid any possible membrane deformation. Further investigation in different geometries of microstructures with proper materials and chemistries could provide a more optimized form of membranes with desired electrochemical properties for higher RED power generation.

3.5. Membrane performance in the RED system

Because the RED system is the reverse process of electrodialysis (ED), many IEMs available on the market designed for ED have been investigated for their performance in the RED system. Only a brief collection of the most common commercial membranes is shown in Table 2, which is based on their reported application in RED systems [26,30]. Apparent desired properties, such as permselectivity and ionic resistance, are listed in Table 2 along with other importance characteristics. The performance of different membrane pairs in specific stacks from the literature is summarized in Table 3. Other related information on stack design and operational parameters are also included.

Generally, more homogeneous membranes are commercially available than heterogeneous ones. For both commercial and tailor-made CEMs, sulfonated groups are universally used as ionogenic groups. Ionogenic groups used in AEMs are more diverse. The thicknesses of these membranes are mostly in the range of 100–200 μm because of limitations in terms of stack thickness and consideration of overall internal resistance of RED cells. For permselectivities, AEMs are less selective than CEMs in general. The permselectivity of AEMs range from 80–90%, whereas the CEMs are mostly above 95%.

Table 3 shows the highest power density reported from experimental data as 2.2 W m^{-2} using commercial membrane pairs (FAS and FKS) [18]. The use of thin spacers (100 μm) is definitely a significant improvement. The effort on enhancing IEM performance also results high power density. The highest power densities of 1.3 W m^{-2} were achieved using custom-made or a mix of custom-made and commercial membranes (SPEEK, PECH, 0.7 wt% Fe_2O_3–SO_4^{2-} sPPO) in all cases [12,14,30]. A comparison that includes information from Tables 2 and 3 reveals that low resistance ($<$ 1.0 $\Omega\,cm^2$) is the key property, which is enhanced by specific design and custom-made membranes. On the other hand, the permselectivity is not that critical (86.5–87.7%) even though the low permselectivity of custom-made membranes is compensated for by very high permselectivity of the other membranes in a pair (ASV: 97%; CMX: 99%). For a pair consisting of both commercial membranes, those with a relatively low resistance (FKD/FAD and FKS/FAS) also resulted in better performance. One exception is the pair (CMV/AMV) that has a relatively high resistance and a mediocre permselectivity and still gives a high power density of 1.11 W m^{-2}. In general, this is in agreement with the discussion in Section 2 and the result of simulation work which determined that low resistance and well-balanced permselectivity are most important in membrane performance [133].

Stack design also affects overall performance when comparing the same pair of membranes used under different stack parameters; however, its effect is limited when thin spacers or higher

flow rates are applied. Consequently, the improvement of membrane properties would definitely be one of the main breakthroughs for the development of a successful RED application.

4. Stack/system design under development

4.1. Ion conductive spacers

Theoretical power output and process efficiency are often affected by the concentration polarization and the spacer shadow effect. Concentration polarization is due to different transference numbers of the ions in the solution and in the membrane, which results in the depletion and the accumulation of ions at the membrane surfaces [22]. This phenomenon can be treated by optimizing the hydrodynamics in a RED stack [50,139]; however, the spacer shadow effect occurring in RED is mostly due to the spacer materials caused by commercially available non-conductive spacers in the RED stack. This effect hinders ion transport from the solution phase to the membrane. The use of ion conductive material for RED spacers is often considered to reduce the shadow effect, allowing more available area for ion transport. Dlugolecki et al. [139] used ion conductive spacers to obtain a significant reduction of the spacer shadow effect. The elimination of the shadow effect led to a large reduction in stack resistance and an increase in power density. Furthermore, such optimization efforts on spacer design (e.g., use of ion conductive spacer) not only contributes to stack resistance reduction but may also help to reduce the effect of polarization [139,140]. Nevertheless, considering that concentration polarization still plays a significant role in overall stack resistance, further efforts to optimize the hydrodynamics and stack design are still required to lessen the concentration polarization effect on power output. Greater energy production with low stack resistance depends on an effective stack design that consists of uniquely tailored spacers and IEMs for RED application.

4.2. Electrochemical couples for RED

The electrode system is one of the key components of the RED setup. In the electrode system, electron transfer reactions allow the transformation of the charge carrier from an ion to an electron and then to a current. Only a few published works have reported an experimental investigation on the electrode material-redox couple system under RED operative conditions. However, Scialdone et al. [141] listed the following considerations for properly selecting suitable electrode systems: low voltage drops at the electrode-solution interphase, the low cost of redox species and electrodes, the high solubility of the redox couple, the chemical and electrochemical stability of redox species, and the physical and chemical stability of electrodes. This paper cannot report on all criteria in practice; however, an Fe(III)–Fe(II) couple warrants coverage. Serial electrolyte combinations such as $FeCl_3/FeCl_2$, $[Fe(CN)_6]^{3-}/[Fe(CN)_6]^{4-}$ and Fe(III)–EDTA/Fe(II)–EDTA have been investigated [52,141] and were found to be unstable under the investigated conditions. $[Fe(CN)_6]^{3-}/[Fe(CN)_6]^{4-}$ proved to be more effective in the absence of light and oxygen by combining with high redox couple concentrations and low current densities at both compact graphite and DSA electrodes. Success using $FeCl_3/FeCl_2$ lies in its stability, which remains constant at acidic pH for long durations at compact graphite electrodes [141]. Despite this success, more research on electrode systems with an RED application are needed to investigate feasible candidates for bench and large-scale stacks with an emphasis on safety, health, technical feasibility, and economics for real application.

4.3. Hybrid process of RED

Various technologies and processes are being combined to explore more synergistic approaches. The hybrid process of RED can maximize productivity and allow for various applications of technologies at a lower capital cost. In this section, various RED-based hybrid processes and their characteristics are reviewed to show the trends in the application of hybrid RED processes.

Reverse osmosis (RO) is one frequently used technique for seawater desalination. In spite of its wide use, RO is still unsatisfactory because of its energy-intensive process. The hybrid process of RO and RED has complementary advantages over stand-alone RO or RED processes. The concentrated brine discharged from the RO process can be fed back to the RED system as concentrated salt water. This brine feed allows for a greater concentration gradient, which enhances the power generation and conversion efficiency of RED [142]. Diluted effluent water from the RED system can be used as a pretreated feed solution for the RO unit, which reduces the energy consumption in the system. This synergistic effect makes RO and RED an ideal combination for effective desalination and brine management with less energy consumption, which provides great advantages over the conventional RO processes [142].

Bioelectrochemical-based systems (BESs) can also be combined with RED to create another form of hybrid technology. BES technologies, such as the microbial fuel cell (MFC), use microorganisms at the bioelectrode (anode) to catalyze the oxidation reaction [143]. BESs help to reduce overpotentials for diverse electrochemical reactions, which also allows for the capture of energy from waste biomass as electricity or biofuels [144,145]. Considering the fact that large electrode overpotential is one of the limiting factors in RED practice (which leads up to a 50% loss in efficiency [52,146]), combining RED with BESs can be beneficial for effective operation. Kim and Logan [143] first proposed a microbial reverse electrodialysis cell (MRC), which contains the RED cell pairs in between MFC electrodes [143]. MRC exhibited three times the voltage (1.2 V) and 6.1 times the power density ($4.3\ W\ m^{-2}$) compared with that of a stand-alone MFC [143]. (Note that in this work the power density of MRC is expressed in $W\ m^{-2}$ of electrode.) In addition, MRC also showed a great potential in harvesting hydrogen gas by using ammonium bicarbonate salts, which are known to be regenerated with heating. Nam et al. [147] demonstrated a system for the production of hydrogen gas based on the concept of salt recovery using a low-grade waste heat source, which is readily available in wastewater treatment plants. This allows for the use of a high salt solution in an RED system for electricity generation as well as hydrogen gas production in MRC.

This section summarized the most important research done in the early development stage of advanced RED application and concluded that hybrid processes of RED offer more opportunities to overcome current limitations of individual systems. More systematic experimental studies should be carried out to validate these RED hybrid processes on the basis of current theoretical findings. The benefits to be obtained from hybrid processes of RED provide great opportunities for further innovation.

5. Conclusions and future directions

Ocean water has become the source of power in membrane-based systems, which can capture energy from its salinity gradient. Although the advantages of harvesting energy using the salinity gradient from seawater and river water are well understood, little attention has been given to the development of new membrane materials and their properties. Specifically for the RED process, the preparation of IEMs and understanding the properties and factors that determine the performance are the most crucial.

This review evaluates potential IEM materials and currently available state-of-the-art RED membranes. The key physicochemical and electrochemical properties of the ideal RED membranes are discussed as well as important performance-determining RED phenomena using experimentally obtained characteristics and theoretical RED models. The importance of membrane development and optimization for the RED application using cost-competitive materials has been stressed in many studies. A successful large-scale energy conversion by RED depends on effective and inexpensive membranes that are uniquely tailored and carefully optimized to specific conditions and solutions for the RED process. In this paper, a number of exemplary materials, namely PVA, PPO, and PVC, were proposed to represent typical low-cost, well-developed, and frequently used IEM materials; however, the overall cost of IEMs will only decrease further as the system advances, which, in turn, will expedite the application of RED as a viable energy conversion technique.

Various innovative methods can be investigated to advance the system as well as to overcome the cost disadvantage. In RED application, better quality membrane products ensure better performance, which often can be achieved by improving the physicochemical structure of the membranes. Many different methods have been demonstrated in the past decade to accomplish this, and we found that the most appropriate ways are as follows: (1) copolymerization, (2) use of a crosslinking agent, (3) formation of a hybrid structure (organic–inorganic), (4) controlling the degree of chemical reactions (e.g., sulfonation and amination), and (5) tailoring the ratio of the polymeric binder or the inorganic filler loading. The design of RED-specific membranes for greater and more efficient power generation should consider certain characteristics. First, the experimental determination and the model calculation clearly recommend membranes with low internal resistance and high permselectivity. The complex relationship between the fixed charge concentration and the water content of the membrane affects the permselectivity and the electrical resistance of the membrane, often leading to an uncertain correlation with RED power density. Well-balanced permselectivity and resistance are preferred with careful optimization, which requires further investigation. The correlation of certain properties with power density may vary depending on the specific membrane materials and the chosen preparation method for synthesizing RED membranes.

In practice, the fouling resistance of membranes can be critical when using natural seawater and river water. For such natural waters, pretreatment may reduce the membrane fouling, or the membrane can also be specifically designed to improve the monovalent ion selectivity and the antifouling properties by altering the membrane structure with a charged coating layer that contains polyelectrolyte. The optimization of key components within the RED system can be supported by theoretical modeling approaches. With further advancement and improvement, the energy capture of RED from salinity gradients will become more practical and effective as a future sustainable energy source.

References

[1] B.E. Logan, M. Elimelech, Membrane-based processes for sustainable power generation using water, Nature 488 (2012) 313–319.
[2] R. Pattle, Production of electric power by mixing fresh and salt water in the hydroelectric pile, Nature 174 (1954) 660.
[3] G.Z. Ramon, B.J. Feinberg, E.M.V. Hoek, Membrane-based production of salinity-gradient power, Energy Environ. Sci. 4 (2011) 4423.
[4] J.W. Post, J. Veerman, H.V.M. Hamelers, G.J.W. Euverink, S.J. Metz, K. Nymeijer, C.J.N. Buisman, Salinity-gradient power: evaluation of pressure-retarded osmosis and reverse electrodialysis, J. Membr. Sci. 288 (2007) 218–230.
[5] V. Shaposhnik, K. Kesore, An early history of electrodialysis with permselective membranes, J. Membr. Sci. 136 (1997) 35–39.
[6] J.N. Weinstein, F.B. Leitz, Electric power from differences in salinity: the dialytic battery, Science 191 (1976) 557.
[7] R.E. Lacey, Energy by reverse electrodialysys, Ocean Eng. 7 (1980) 1–47.
[8] J. Jagur-Grodzinski, R. Kramer, Novel process for direct conversion of free energy of mixing into electric power, Ind. Eng. Chem. Process Design Dev. 25 (1986) 443–449.
[9] M. Turek, B. Bandura, Renewable energy by reverse electrodialysis, Desalination 205 (2007) 67–74.
[10] A. Daniilidis, R. Herber, D.A. Vermaas, Upscale potential and financial feasibility of a reverse electrodialysis power plant, Appl. Energy 119 (2014) 257–265.
[11] M. Elimelech, W.A. Phillip, The future of seawater desalination: energy, technology, and the environment, Science 333 (2011) 712–717.
[12] J.G. Hong, Y. Chen, Nanocomposite reverse electrodialysis (RED) ion-exchange membranes for salinity gradient power generation, J. Membr. Sci. 460 (2014) 139–147.
[13] E. Guler, Y.L. Zhang, M. Saakes, K. Nijmeijer, Tailor-made anion-exchange membranes for salinity gradient power generation using reverse electrodialysis, Chemsuschem 5 (2012) 2262–2270.
[14] E. Guler, R. Elizen, M. Saakes, K. Nijmeijer, Micro-structured membranes for electricity generation by reverse electrodialysis, J. Membr. Sci. 458 (2014) 136–148.
[15] J.G. Hong, Y. Chen, Evaluation of electrochemical properties and reverse electrodialysis performance for porous cation exchange membranes with sulfate-functionalized iron oxide, J. Membr. Sci. 473 (2015) 210–217.
[16] R.K. Nagarale, G.S. Gohil, V.K. Shahi, Recent developments on ion-exchange membranes and electro-membrane processes, Adv. Colloid Interface Sci. 119 (2006) 97–130.
[17] T. Sata, Ion Exchange Membranes: Preparation, Characterization, Modification and Application, The Royal Society of Chemistry, Cambridge, 2004.
[18] D.A. Vermaas, M. Saakes, K. Nijmeijer, Doubled power density from salinity gradients at reduced intermembrane distance, Environ. Sci. Technol. 45 (2011) 7089–7095.
[19] D.L. Feldheim, Del R. Lawson, Charles R. Martin, Influence of the sulfonate countercation on the thermal stability of Nafion perfluorousulfonate membranes, J. Polymer Sci.: Part B: Polymer Phys. 31 (1993) 953–957.
[20] N.P. Brandon, S. Skinner, B.C.H. Steele, Recent advances in materials for fuel cells, Annu. Rev. Mater. Res. 33 (2003) 183–213.
[21] K. Kontturi, L. Murtomäki, J.A. Manzanares, Ionic Transport Processes in Electrochemistry and Membrane Science, Oxford University Press, New York, 2008.
[22] H. Strathmann, Ion-Exchange Membrane Separation Processes, Elsevier Science Limited, Amsterdam, 2004.
[23] H. Strathmann, ScienceDirect (Online service), Ion-exchange membrane separation processes, in: Membrane Science and Technology Series, Elsevier, Amsterdam, Boston, 2004, p. xi, 348 pp.
[24] F. Helfer, C. Lemckert, Y.G. Anissimov, Osmotic power with pressure retarded osmosis: theory, performance and trends – a review, J. Membr. Sci. 453 (2014) 337–358.
[25] S. Koter, P. Piotrowski, J. Kerres, Comparative investigations of ion-exchange membranes, J. Membr. Sci. 153 (1999) 83–90.
[26] P. Dlugolecki, K. Nymeijer, S. Metz, M. Wessling, Current status of ion exchange membranes for power generation from salinity gradients, J. Membr. Sci. 319 (2008) 214–222.
[27] G.M. Geise, M.A. Hickner, B.E. Logan, Ionic resistance and permselectivity tradeoffs in anion exchange membranes, ACS Appl. Mater. Interfaces 5 (2013) 10294–10301.
[28] C. Klaysom, S.H. Moon, B.P. Ladewig, G.Q.M. Lu, L.Z. Wang, Preparation of porous ion-exchange membranes (IEMs) and their characterizations, J. Membr. Sci. 371 (2011) 37–44.
[29] A.H. Galama, J.W. Post, M.A.C. Stuart, P.M. Biesheuvel, Validity of the Boltzmann equation to describe Donnan equilibrium at the membrane–solution interface, J. Membr. Sci. 442 (2013) 131–139.
[30] E. Guler, R. Elizen, D. Vermaas, M. Saakes, K. Nijmeijer, Performance-determining membrane properties in reverse electrodialysis, J. Membr. Sci. (2013).
[31] M. Kumar, S. Singh, V.K. Shahi, Cross-linked poly(vinyl alcohol)–poly(acrylonitrile-co-2-dimethylamino ethylmethacrylate) based anion-exchange membranes in aqueous media, J. Phys. Chem. B 114 (2010) 198–206.
[32] A.R. Khare, N.A. Peppas, Swelling deswelling of anionic copolymer gels, Biomaterials 16 (1995) 559–567.
[33] H. Strathmann, A. Grabowski, G. Eigenberger, Ion-exchange membranes in the chemical process industry, Ind. Eng. Chem. Res. 52 (2013) 10364–10379.
[34] S. Nouri, L. Dammak, G. Bulvestre, B. Auclair, Comparison of three methods for the determination of the electrical conductivity of ion-exchange polymers, Eur. Polymer J. 38 (2002) 1907–1913.
[35] G.M. Geise, A.J. Curtis, M.C. Hatzell, M.A. Hickner, B.E. Logan, Salt concentration differences alter membrane resistance in reverse electrodialysis stacks, Environ. Sci. Technol. Lett. 1 (2013) 36–39.
[36] P. Dlugolecki, B. Anet, S.J. Metz, K. Nijmeijer, M. Wessling, Transport limitations in ion exchange membranes at low salt concentrations, J. Membr. Sci. 346 (2010) 163–171.
[37] P. Dlugolecki, A. Gambier, K. Nijmeijer, M. Wessling, Practical potential of reverse electrodialysis as process for sustainable energy generation, Environ. Sci. Technol. 43 (2009) 6888–6894.

[38] P. Dlugolecki, P. Ogonowski, S.J. Metz, M. Saakes, K. Nijmeijer, M. Wessling, On the resistances of membrane, diffusion boundary layer and double layer in ion exchange membrane transport, J. Membr. Sci. 349 (2010) 369–379.
[39] A.H. Galama, D.A. Vermaas, J. Veerman, M. Saakes, H.H.M. Rijnaarts, J.W. Post, Membrane resistance: the effect of salinity gradients over a cation exchange membrane, J. Membr. Sci. 467 (2014) 279–291.
[40] P. Sistat, G. Pourcelly, Chronopotentiometric response of an ion-exchange membrane in the underlimiting current-range. Transport phenomena within the diffusion layers, J. Membr. Sci. 123 (1997) 121–131.
[41] R. Audinos, G. Pichelin, Characterization of electrodialysis membranes by chronopotentiometry, Desalination 68 (1988) 251–263.
[42] A.A. Moya, P. Sistat, Chronoamperometric response of ion-exchange membrane systems, J. Membr. Sci. 444 (2013) 412–419.
[43] J.S. Park, J.H. Choi, J.J. Woo, S.H. Moon, An electrical impedance spectroscopic (EIS) study on transport characteristics of ion-exchange membrane systems, J. Colloid Interface Sci. 300 (2006) 655–662.
[44] L.V. Karpenko, O.A. Demina, G.A. Dvorkina, S.B. Parshikov, C. Larchet, B. Auclair, N.P. Berezina, Comparative study of methods used for the determination of electroconductivity of ion-exchange membranes, Russ. J. Electrochem. 37 (2001) 287–293.
[45] V.V. Nikonenko, A.E. Kozmai, Electrical equivalent circuit of an ion-exchange membrane system, Electrochim. Acta 56 (2011) 1262–1269.
[46] F.G. Helfferich, Ion Exchange, McGraw-Hill, New York, 1962.
[47] J. Veerman, J.W. Post, M. Saakes, S.J. Metz, G.J. Harmsen, Reducing power losses caused by ionic shortcut currents in reverse electrodialysis stacks by a validated model, J. Membr. Sci. 310 (2008) 418–430.
[48] A. Grabowski, G.Q. Zhang, H. Strathmann, G. Eigenberger, The production of high purity water by continuous electrodeionization with bipolar membranes: Influence of the anion-exchange membrane permselectivity, J. Membr. Sci. 281 (2006) 297–306.
[49] H. Strathmann, Electrodialysis, a mature technology with a multitude of new applications, Desalination 264 (2010) 268–288.
[50] J. Veerman, M. Saakes, S. Metz, G. Harmsen, Reverse electrodialysis: performance of a stack with 50 cells on the mixing of sea and river water, J. Membr. Sci. 327 (2009) 136–144.
[51] J.W. Post, H.V.M. Hamelers, C.J.N. Buisman, Energy recovery from controlled mixing salt and fresh water with a reverse electrodialysis system, Environ. Sci. Technol. 42 (2008) 5785–5790.
[52] J. Veerman, M. Saakes, S. Metz, G. Harmsen, Reverse electrodialysis: evaluation of suitable electrode systems, J. Appl. Electrochem. 40 (2010) 1461–1474.
[53] S. Pawlowski, P. Sistat, J.G. Crespo, S. Velizarov, Mass transfer in reverse electrodialysis: flow entrance effects and diffusion boundary layer thickness, J. Membr. Sci. 471 (2014) 72–83.
[54] K.S. Kim, W. Ryoo, M.S. Chun, G.Y. Chung, Simulation of enhanced power generation by reverse electrodialysis stack module in serial configuration, Desalination 318 (2013) 79–87.
[55] F. Suda, T. Matsuo, D. Ushioda, Transient changes in the power output from the concentration difference cell (dialytic battery) between seawater and river water, Energy 32 (2007) 165–173.
[56] E. Brauns, Salinity gradient power by reverse electrodialysis: effect of model parameters on electrical power output, Desalination 237 (2009) 378–391.
[57] E. Brauns, Towards a worldwide sustainable and simultaneous large-scale production of renewable energy and potable water through salinity gradient power by combining reversed electrodialysis and solar power? Desalination 219 (2008) 312–323.
[58] H.P. Gregor, M.A. Peterson, Electrodialytic polarization of ion-exchange membrane systems, J. Phys. Chem. 68 (1964) 2201–2205.
[59] N. Lakshmin, Transport phenomena in artificial membranes, Chem. Rev. 65 (1965) 491–565.
[60] V.M. Barragan, C. Ruiz-Bauza, Current–voltage curves for ion-exchange membranes: a method for determining the limiting current density, J. Colloid Interface Sci. 205 (1998) 365–373.
[61] D.A. Vermaas, M. Saakes, K. Nijmeijer, Enhanced mixing in the diffusive boundary layer for energy generation in reverse electrodialysis, J. Membr. Sci. 453 (2014) 312–319.
[62] D.A. Vermaas, E. Guler, M. Saakes, K. Nijmeijer, Theoretical power density from salinity gradients using reverse electrodialysis, Energy Procedia 20 (2012) 170–184.
[63] D.A. Vermaas, M. Saakes, K. Nijmeijer, Early detection of preferential channeling in reverse electrodialysis, Electrochim. Acta 117 (2014) 9–17.
[64] L. Gurreri, A. Tamburini, A. Cipollina, G. Micale, M. Ciofalo, CFD simulation of mass transfer phenomena in spacer filled channels for reverse electrodialysis applications, Chem. Eng. Trans. 32 (2013) 1879–1884.
[65] M. Tedesco, A. Cipollina, A. Tamburini, I.D.L. Bogle, G. Micale, A simulation tool for analysis and design of reverse electrodialysis using concentrated brines, Chem. Eng. Res. Design (2014).
[66] J. Veerman, M. Saakes, S.J. Metz, G.J. Harmsen, Electrical power from sea and river water by reverse electrodialysis: a first step from the laboratory to a real power plant, Environ. Sci. Technol. 44 (2010) 9207–9212.
[67] J. Veerman, R. De Jong, M. Saakes, S. Metz, G. Harmsen, Reverse electrodialysis: comparison of six commercial membrane pairs on the thermodynamic efficiency and power density, J. Membr. Sci. 343 (2009) 7–15.
[68] J.W. Post, H.V.M. Hamelers, C.J.N. Buisman, Influence of multivalent ions on power production from mixing salt and fresh water with a reverse electrodialysis system, J. Membr. Sci. 330 (2009) 65–72.
[69] J.G. Hong, W. Zhang, J. Luo, Y. Chen, Modeling of power generation from the mixing of simulated saline and freshwater with a reverse electrodialysis system: the effect of monovalent and multivalent ions, Appl. Energy 110 (2013) 244–251.
[70] J.G. Hong, W. Zhang, J. Luo, Y. Chen, Corrigendum to "Modeling of power generation from the mixing of simulated saline and freshwater with a reverse electrodialysis system: the effect of monovalent and multivalent ions", Appl. Energy 110 (2013) 244–251 (Applied Energy (2014)).
[71] D.A. Vermaas, J. Veerman, M. Saakes, K. Nijmeijer, Influence of multivalent ions on renewable energy generation in reverse electrodialysis, Energy Environ. Sci. 7 (2014) 1434–1445.
[72] M. Zhang, H.K. Kim, E. Chalkova, F. Mark, S.N. Lvov, T.M. Chung, New polyethylene based anion exchange membranes (PE–AEMs) with high ionic conductivity, Macromolecules 44 (2011) 5937–5946.
[73] T.W. Xu, Ion exchange membranes: state of their development and perspective, J. Membr. Sci. 263 (2005) 1–29.
[74] B.D. Gupta, A. Chapiro, Preparation of ion-exchange membranes by grafting acrylic acid into pre-irradiated polymer films–2. Grafting into teflon-FEP, Eur. Polymer J. 25 (1989) 1145–1148.
[75] S. Aouadj, A. Chapiro, Preparation of hydrophilic membranes by grafting acrylic acid onto pre-irradiated teflon-FEP films, Die Angew. Makromol. Chem. 235 (1996) 73–80.
[76] E.S.A. Hegazy, N. Taher, A. Ebaid, Preparation and some properties of hydrophilic membranes obtained by radiation grafting of methacrylic acid onto fluorinated polymers, J. Appl. Polymer Sci. 41 (1990) 2637–2647.
[77] K. Saito, K. Saito, K. Sugita, M. Tamada, T. Sugo, Convection-aided collection of metal ions using chelating porous flat-sheet membranes, J. Chromatogr. A 954 (2002) 277–283.
[78] T.W. Xu, W.H. Yang, B.L. He, Effect of solvent composition on the sulfonation degree of poly(phenylene oxide) (PPO), Chin. J. Polymer Sci. 20 (2002) 53–57.
[79] E.N. Komkova, D.F. Stamatialis, H. Strathmann, M. Wessling, Anion-exchange membranes containing diamines: preparation and stability in alkaline solution, J. Membr. Sci. 244 (2004) 25–34.
[80] R.S.L. Yee, R.A. Rozendal, K. Zhang, B.P. Ladewig, Cost effective cation exchange membranes: a review, Chem. Eng. Res. Des. 90 (2012) 950–959.
[81] C. Zhao, W. Ma, W. Sun, H. Na, Preparation of anion exchange membrane based on homogeneous quaternization of bromomethylated poly (arylene ether sulfone), J. Appl. Polymer Sci. (2013).
[82] M.R. Hibbs, C.H. Fujimoto, C.J. Cornelius, Synthesis and characterization of poly (phenylene)-based anion exchange membranes for alkaline fuel cells, Macromolecules 42 (2009) 8316–8321.
[83] R. Vinodh, A. Ilakkiya, S. Elamathi, D. Sangeetha, A novel anion exchange membrane from polystyrene (ethylene butylene) polystyrene: synthesis and characterization, Mater. Sci. Eng.: B 167 (2010) 43–50.
[84] H. Herman, R.C.T. Slade, J.R. Varcoe, The radiation-grafting of vinylbenzyl chloride onto poly(hexafluoropropylene-co-tetrafluoroethylene) films with subsequent conversion to alkaline anion-exchange membranes: optimisation of the experimental conditions and characterisation, J. Membr. Sci. 218 (2003) 147–163.
[85] T. Sata, Y. Yamane, K. Matsusaki, Preparation and properties of anion exchange membranes having pyridinium or pyridinium derivatives as anion exchange groups, J. Polymer Sci. Part A: Polymer Chem. 36 (1998) 49–58.
[86] Q.G. Zhang, Q.L. Liu, A.M. Zhu, Y. Xiong, L. Ren, Pervaporation performance of quaternized poly (vinyl alcohol) and its crosslinked membranes for the dehydration of ethanol, J. Membr. Sci. 335 (2009) 68–75.
[87] T. Sata, M. Tsujimoto, T. Yamaguchi, K. Matsusaki, Change of anion exchange membranes in an aqueous sodium hydroxide solution at high temperature, J. Membr. Sci. 112 (1996) 161–170.
[88] C.-P. Liu, C.-A. Dai, C.-Y. Chao, S.-J. Chang, Novel proton exchange membrane based on crosslinked poly (vinyl alcohol) for direct methanol fuel cells, J. Power Sources 249 (2014) 285–298.
[89] J.W. Rhim, H.B. Park, C.S. Lee, J.H. Jun, D.S. Kim, Y.M. Lee, Crosslinked poly (vinyl alcohol) membranes containing sulfonic acid group: proton and methanol transport through membranes, J. Membr. Sci. 238 (2004) 143–151.
[90] J. Zhang, J.L. Qiao, G.P. Jiang, L.L. Liu, Y.Y. Liu, Cross-linked poly(vinyl alcohol)/poly (diallyldimethylammonium chloride) as anion-exchange membrane for fuel cell applications, J. Power Sources 240 (2013) 359–367.
[91] M. Wilhelm, M. Jeske, R. Marschall, W.L. Cavalcanti, P. Tölle, C. Köhler, D. Koch, T. Frauenheim, G. Grathwohl, J. Caro, M. Wark, New proton conducting hybrid membranes for HT-PEMFC systems based on polysiloxanes and SO_3H-functionalized mesoporous Si-MCM-41 particles, J. Membr. Sci. 316 (2008) 164–175.
[92] B.P. Tripathi, V.K. Shahi, Organic–inorganic nanocomposite polymer electrolyte membranes for fuel cell applications, Prog. Polymer Sci. 36 (2011) 945–979.
[93] Y.H. Wu, J.W. Hao, C.M. Wu, F.L. Mao, T.W. Xu, Cation exchange PVA/SPPO/SiO_2 membranes with double organic phases for alkali recovery, J. Membr. Sci. 423 (2012) 383–391.
[94] C.C. Yang, S.J. Chiu, W.C. Chien, S.S. Chiu, Quaternized poly(vinyl alcohol)/alumina composite polymer membranes for alkaline direct methanol fuel cells, J. Power Sources 195 (2010) 2212–2219.
[95] S. Yun, H. Im, Y. Heo, J. Kim, Crosslinked sulfonated poly(vinyl alcohol)/sulfonated multi-walled carbon nanotubes nanocomposite membranes for direct methanol fuel cells, J. Membr. Sci. 380 (2011) 208–215.

[96] T.W. Xu, D. Wu, L. Wu, Poly(2,6-dimethyl-1,4-phenylene oxide) (PPO) – a versatile starting polymer for proton conductive membranes (PCMs), Prog. Polymer Sci. 33 (2008) 894–915.
[97] T.W. Xu, W.H. Yang, B.L. He, Ionic conductivity threshold in sulfonated poly (phenylene oxide) matrices: a combination of three-phase model and percolation theory, Chem. Eng. Sci. 56 (2001) 5343–5350.
[98] Y. Wu, C. Wu, T. Xu, X. Lin, Y. Fu, Novel silica/poly(2,6-dimethyl-1,4-phenylene oxide) hybrid anion-exchange membranes for alkaline fuel cells: effect of heat treatment, J. Membr. Sci. 338 (2009) 51–60.
[99] S.M. Hosseini, A. Gholami, S.S. Madaeni, A.R. Moghadassi, A.R. Hamidi, Fabrication of (polyvinyl chloride/cellulose acetate) electrodialysis heterogeneous cation exchange membrane: characterization and performance in desalination process, Desalination 306 (2012) 51–59.
[100] M. Arsalan, M.M.A. Khan, Rafiuddin, A comparative study of theoretical, electrochemical and ionic transport through PVC based $Cu_3(PO_4)_2$ and polystyrene supported $Ni_3(PO_4)_2$ composite ion exchange porous membranes, Desalination 318 (2013) 97–106.
[101] J. Hu, C.X. Zhang, J. Cong, H. Toyoda, M. Nagatsu, Y.D. Meng, Plasma-grafted alkaline anion-exchange membranes based on polyvinyl chloride for potential application in direct alcohol fuel cell, J. Power Sources 196 (2011) 4483–4490.
[102] N. Gizli, S. Cinarli, M. Demircioglu, Characterization of poly(vinylchloride) (PVC) based cation exchange membranes prepared with ionic liquid, Sep. Purif. Technol. 97 (2012) 96–107.
[103] S.M. Hosseini, S.S. Madaeni, A.R. Heidari, A. Amirimehr, Preparation and characterization of ion-selective polyvinyl chloride based heterogeneous cation exchange membrane modified by magnetic iron-nickel oxide nanoparticles, Desalination 284 (2012) 191–199.
[104] J.W. Post, H.V.M. Hamelers, C.J.N. Buisman, Influence of multivalent ions on power production from mixing salt and fresh water with a reverse electrodialysis system, J. Membr. Sci. 330 (2009) 65–72.
[105] E. Guler, W. van Baak, M. Saakes, K. Nijmeijer, Monovalent-ion-selective membranes for reverse electrodialysis, J. Membr. Sci. 455 (2014) 254–270.
[106] S. Siracusano, V. Baglio, M. Navarra, S. Panero, V. Antonucci, A. Aricò, Investigation of composite nafion/sulfated zirconia membrane for solid polymer electrolyte electrolyzer applications, Int. J. Electrochem. Sci. 7 (2012).
[107] X.T. Zuo, S.L. Yu, X. Xu, R.L. Bao, J. Xu, W.M. Qu, Preparation of organic–inorganic hybrid cation-exchange membranes via blending method and their electrochemical characterization, J. Membr. Sci. 328 (2009) 23–30.
[108] Z. Wang, H.L. Tang, H.J. Zhang, M. Lei, R. Chen, P. Xiao, M. Pan, Synthesis of Nafion/CeO_2 hybrid for chemically durable proton exchange membrane of fuel cell, J. Membr. Sci. 421 (2012) 201–210.
[109] L.L. Sun, S.L. Wang, W. Jin, H.Y. Hou, L.H. Jiang, G.Q. Sun, Nano-sized Fe_2O_3–SO_4^{2-} solid superacid composite Nafion (R) membranes for direct methanol fuel cells, Int. J. Hydrogen Energy 35 (2010) 12461–12468.
[110] R.K. Nagarale, V.K. Shahi, R. Rangarajan, Preparation of polyvinyl alcohol–silica hybrid heterogeneous anion-exchange membranes by sol–gel method and their characterization, J. Membr. Sci. 248 (2005) 37–44.
[111] Y.G. Jeong, H.S. Park, D.W. Seo, S.W. Choi, W.G. Kim, Nano composite membranes of sulfonated poly (2, 6-dimethyl-1, 4-phenylene oxide)/poly (2, 6-diphenyl-1, 4-phenylene oxide) copolymer and SiO_2 for fuel cell application, Adv. Mater. Res. 26 (2007) 835–838.
[112] R.K. Nagarale, G.S. Gohil, V.K. Shahi, R. Rangarajan, Organic–inorganic hybrid membrane: thermally stable cation-exchange membrane prepared by the sol–gel method, Macromolecules 37 (2004) 10023–10030.
[113] F.H. Wang, Z. Lu, H. Zhu, X.W. Zhang, Z.J. Guo, Y.S. Wei, Preparation and characterization of nafion/sulfonated SiO_2 molecular sieve composite membranes, Compos. Interfaces 18 (2011) 237–249.
[114] C.C. Ke, X.J. Li, Q.A. Shen, S.G. Qu, Z.G. Shao, B.L. Yi, Investigation on sulfuric acid sulfonation of in-situ sol–gel derived Nafion/SiO_2 composite membrane, Int. J. Hydrogen Energy 36 (2011) 3606–3613.
[115] C. Klaysom, R. Marschall, L.Z. Wang, B.P. Ladewig, G.Q.M. Lu, Synthesis of composite ion-exchange membranes and their electrochemical properties for desalination applications, J. Mater. Chem. 20 (2010) 4669–4674.
[116] Y.H. Su, Y.L. Liu, Y.M. Sun, J.Y. Lai, D.M. Wang, Y. Gao, B.J. Liu, M.D. Guiver, Proton exchange membranes modified with sulfonated silica nanoparticles for direct methanol fuel cells, J. Membr. Sci. 296 (2007) 21–28.
[117] C.H. Lee, K.A. Min, H.B. Park, Y.T. Hong, B.O. Jung, Y.M. Lee, Sulfonated poly (arylene ether sulfone)–silica nanocomposite membrane for direct methanol fuel cell (DMFC), J. Membr. Sci. 303 (2007) 258–266.
[118] J.Y. Kim, S. Mulmi, C.H. Lee, H.B. Park, Y.S. Chung, Y.M. Lee, Preparation of organic–inorganic nanocomposite membrane using a reactive polymeric dispersant and compatibilizer: proton and methanol transport with respect to nano-phase separated structure, J. Membr. Sci. 283 (2006) 172–181.
[119] C.M. Wu, T.W. Xu, M. Gong, W.H. Yang, Synthesis and characterizations of new negatively charged organic-inorganic hybrid materials Part II. Membrane preparation and characterizations, J. Membr. Sci. 247 (2005) 111–118.
[120] A. Rahimpour, S.S. Madaeni, A.H. Taheri, Y. Mansourpanah, Coupling TiO_2 nanoparticles with UV irradiation for modification of polyethersulfone ultrafiltration membranes, J. Membr. Sci. 313 (2008) 158–169.
[121] J.F. Li, Z.L. Xu, H. Yang, L.Y. Yu, M. Liu, Effect of TiO_2 nanoparticles on the surface morphology and performance of microporous PES membrane, Appl. Surf. Sci. 255 (2009) 4725–4732.
[122] Z. Wu, G. Sun, W. Jin, H. Hou, S. Wang, Q. Xin, Nafion® and nano-size TiO_2–SO_4^{2-} solid superacid composite membrane for direct methanol fuel cell, J. Membr. Sci. 313 (2008) 336–343.
[123] V. Baglio, A.S. Arico, A. Di Blasi, V. Antonucci, P.L. Antonucci, S. Licoccia, E. Traversa, F.S. Fiory, Nafion–TiO_2 composite DMFC membranes: physico-chemical properties of the filler versus electrochemical performance, Electrochim. Acta 50 (2005) 1241–1246.
[124] M. Sairam, M.B. Patil, R.S. Veerapur, S.A. Patil, T.M. Aminabhavi, Novel dense poly(vinyl alcohol)–TiO_2 mixed matrix membranes for pervaporation separation of water–isopropanol mixtures at 30 degrees C, J. Membr. Sci. 281 (2006) 95–102.
[125] W. Li, X. Sun, C. Wen, H. Lu, Z. Wang, Preparation and characterization of poly (vinylidene fluoride)/TiO_2 hybrid membranes, Front. Environ. Sci. Eng. 7 (2013) 492–502.
[126] S. Pourjafar, A. Rahimpour, M. Jahanshahi, Synthesis and characterization of PVA/PES thin film composite nanofiltration membrane modified with TiO_2 nanoparticles for better performance and surface properties, J. Ind. Eng. Chem. 18 (2012) 1398–1405.
[127] W. Apichatachutapan, R. Moore, K.A. Mauritz, Asymmetric nafion/(zirconium oxide) hybrid membranes via in situ sol–gel chemistry, J. Appl. Polymer Sci. 62 (1996) 417–426.
[128] Y.F. Zhai, H.M. Zhang, J.W. Hu, B.L. Yi, Preparation and characterization of sulfated zirconia(SO_4^{2-}/ZrO_2)/Nafion composite membranes for PEMFC operation at high temperature/low humidity, J. Membr. Sci. 280 (2006) 148–155.
[129] A. Bottino, G. Capannelli, A. Comite, Preparation and characterization of novel porous PVDF–ZrO_2 composite membranes, Desalination 146 (2002) 35–40.
[130] A. Sacca, I. Gatto, A. Carbone, R. Pedicini, E. Passalacqua, ZrO2–Nafion composite membranes for polymer electrolyte fuel cells (PEFCs) at intermediate temperature, J. Power Sources 163 (2006) 47–51.
[131] M.A. Navarra, C. Abbati, F. Croce, B. Scrosati, Temperature-dependent performances of a fuel cell using a superacid zirconia-doped Nafion polymer electrolyte, Fuel Cells 9 (2009) 222–225.
[132] D.A. Vermaas, M. Saakes, K. Nijmeijer, Power generation using profiled membranes in reverse electrodialysis, J. Membr. Sci. 385-386 (2011) 234–242.
[133] N.Y. Yip, D.A. Vermaas, K. Nijmeijer, M. Elimelech, Thermodynamic, energy efficiency, and power density analysis of reverse electrodialysis power generation with natural salinity gradients, Environ. Sci. Technol. 48 (2014) 4925–4936.
[134] A. Elattar, A. Elmidaoui, N. Pismenskaia, C. Gavach, G. Pourcelly, Comparison of transport properties of monovalent anions through anion-exchange membranes, J. Membr. Sci. 143 (1998) 249–261.
[135] E. Volodina, N. Pismenskaya, V. Nikonenko, C. Larchet, G. Pourcelly, Ion transfer across ion-exchange membranes with homogeneous and heterogeneous surfaces, J. Colloid Interface Sci. 285 (2005) 247–258.
[136] J.N. Weinstein, F.B. Leitz, Electric-power from difference in salinity – dialytic battery, Science 191 (1976) 557–559.
[137] R. Audinos, Inverse electrodialysis. Study of electric energy obtained starting with two solutions of different salinity, J. Power Sources 10 (1983) 203–217.
[138] M. Turek, B. Bandura, Renewable energy by reverse electrodialysis, Desalination 205 (2007) 67–74.
[139] P. Dlugolecki, J. Dabrowska, K. Nijmeijer, M. Wessling, Ion conductive spacers for increased power generation in reverse electrodialysis, J. Membr. Sci. 347 (2010) 101–107.
[140] O. Kedem, Reduction of polarization in electrodialysis by ion-conducting spacers, Desalination 16 (1975) 105–118.
[141] O. Scialdone, C. Guarisco, S. Grispo, A. Angelo, A. Galia, Investigation of electrode material–redox couple systems for reverse electrodialysis processes. Part I: Iron redox couples, J. Electroanal. Chem. 681 (2012) 66–75.
[142] W. Li, W.B. Krantz, E.R. Cornelissen, J.W. Post, A.R. Verliefde, C.Y. Tang, A novel hybrid process of reverse electrodialysis and reverse osmosis for low energy seawater desalination and brine management, Appl. Energy 104 (2013) 592–602.
[143] Y. Kim, B.E. Logan, Microbial reverse electrodialysis cells for synergistically enhanced power production, Environ. Sci. Technol. 45 (2011) 5834–5839.
[144] B.E. Logan, K. Rabaey, Conversion of wastes into bioelectricity and chemicals by using microbial electrochemical technologies, Science 337 (2012) 686–690.
[145] H.V. Hamelers, A. Ter Heijne, T.H. Sleutels, A.W. Jeremiasse, D.P. Strik, C.J. Buisman, New applications and performance of bioelectrochemical systems, Appl. Microbiol. Biotechnol. 85 (2010) 1673–1685.
[146] Y. Kim, B.E. Logan, Hydrogen production from inexhaustible supplies of fresh and salt water using microbial reverse-electrodialysis electrolysis cells, Proc. Natl. Acad. Sci. 108 (2011) 16176–16181.
[147] J.-Y. Nam, R.D. Cusick, Y. Kim, B.E. Logan, Hydrogen generation in microbial reverse-electrodialysis electrolysis cells using a heat-regenerated salt solution, Environ. Sci. Technol. 46 (2012) 5240–5246.